Unintended Consequences of Environmental Regulation of Maritime Shipping: Carbon Leakage to Air Shipping*

Volodymyr Lugovskyy† Alexandre Skiba‡ David Terner§

January 15, 2023

Abstract

We evaluate the impact of the expected International Maritime Organization 2023 regulation (henceforth IMO2023) that caps CO_2 emissions from global maritime shipping. Focusing on US imports—where we use detailed vessel, route, emissions, speed, and trade data—we structurally estimate an import demand model with vessel- and air-delivered imports. We show that IMO2023 will cause demand substitution towards more carbon-intensive air transport to the point that *total* transport-related CO_2 emissions increase. Furthermore, we show that subsidizing fuel for vessels will lower combined air and vessel emissions.

*We are grateful for the excellent feedback provided by Tibor Besedeš, David Hummels, Sam Kortum, Ahmad Lashkaripor, Joseph Shapiro, Joshua Graff Zivin, Woan Foong Wong, Bruce Blonigen, Anca Cristea, Phillip Economides and the participants at (the): University of Oregon Economics Seminar (Fall 2022); Midwest Macroeconomics Meetings (Fall 2022); Empirical Investigations in International Trade (Fall 2022); Midwest Economic Theory and International Trade Conference (Fall 2022); NERA Economic Consulting (Fall 2022); Indiana University Microeconomics Workshop (Fall 2022); Midwest Economic Theory and International Trade Conference (Spring 2022); Indiana University Trade Seminar (Spring 2022); and, Southern Economics Association Meetings (Fall 2021). We thank BlueWater Reporting for providing access to their data on the maritime liner routes and carrier composition. All mistakes are our own.

†Department of Economics, Indiana University, Wylie Hall Rm 301, 100 S. Woodlawn, Bloomington, IN 47405-7104; e-mail: vlugovsk@iu.edu

‡Department of Economics, University of Wyoming; e-mail: askiba@uwyo.edu

§Department of Economics, Indiana University, Wylie Hall Rm 101, 100 S. Woodlawn, Bloomington, IN 47405-7104; e-mail: dmterner@iu.edu

1 Introduction

The United Nations (UN) declared global decarbonization one of its top priorities. As recently stated by Antonio Guterres, Secretary-General of the UN, "Making peace with nature...must be the top, top priority for everyone, everywhere" (Guterres, 2020). Pursuant to this agenda, one of the UN's specialized agencies, the International Maritime Organization (IMO), has been tasked to facilitate maritime shipping decarbonization. Maritime shipping accounts for 1 billion tons of carbon dioxide annually—around 3% of global anthropogenic CO_2 emissions. These emissions are projected to grow further by between 50% and 250% by 2050.[1] To combat this alarming trend, the agency adopted its Initial IMO Strategy on Reduction of GHG Emissions. This regulatory framework attempts to restrict CO_2 emissions from maritime transportation starting in 2023. Therefore, we refer to all regulations and policy changes envisioned by the IMO as IMO2023.[2] IMO2023's goal is to provide increasingly stringent standards towards 2050, with the ambition to reduce CO_2 emissions per transport work by 40% of 2008 levels by 2030 and by 50% by 2050.

As with all public policy, IMO2023 will have its intended and unintended consequences. This paper utilizes a structural model of international shipping and detailed data on vessels, routes, and trade to analyze both sets of consequences. In economics, starting with Pigou (1920), government intervention is a textbook recipe for dealing with environmental externalities; government intervention forces producers to internalize the external cost of pollution, thus mitigating the consequences of market failure. However, the effects of regulation become more complex if regulating one market leads to increased pollution *leakage* within another market. This leakage concern has been studied extensively in the context of geographic markets, such as countries[3] or U.S. counties (e.g., Becker and Henderson, 2000; Greenstone, 2002).

[1] The Third IMO Green House Gas (GHG) Study, 2014.

[2] Emission threshold policies can be traced back to the Initial IMO Strategy on reduction of the GHG adopted in April 2018 (IMO Resolution MEPC.304(72)), which was later extended with new regulations adopted in 2021 (see IMO Resolutions MEPC.335(76), MEPC.336(76), MEPC.337(76), MEPC.338(76)).

[3] There is a large body of literature on trade and environmental regulations, which focuses on environmental aspects of trade, including international leakage and free riding across countries. A very incomplete list of papers in this literature includes Markusen (1975); Copeland (1996); Elliott et al. (2010); Hanna (2010); Copeland et al. (2022); Tanaka et al. (2022); Nordhaus (2015); Farrokhi and Lashkaripour (2021); Kortum and Weisbach (2021).

In this paper, we stress the extent of a different, previously less explored, and potentially far more damaging type of pollution leakage: *inter-modal leakage* from ocean to air freight transportation. That is, by imposing more stringent environmental regulations only on ocean transportation, IMO2023 will push demand for imports away from maritime transportation and towards air freight. This unintended consequence of IMO2023 will be especially severe given that, as highlighted by the previous research (Cristea et al., 2013; Shapiro, 2016), air transportation is up to two orders of magnitude more carbon-intensive than containerized maritime transportation.[4] This vast difference in carbon efficiency between the target regulated market (maritime transportation) and the leakage destination (air transportation) is unprecedented. Therefore, any leakage may not just undermine the effect of regulation, as in case of some other within-industry leakages[5], but can even overturn it, increasing the overall emissions, i.e., in a *Green Paradox*.

Is it possible to quantify the extent of IMO2023 inter-sectoral pollution leakage between the two modes of transportation? In this paper, we attempt exactly that by evaluating the short-run, partial equilibrium effects of IMO2023 on pollution caused by transporting U.S. imports by containerized vessels (i.e., liner shipping) and airplanes. Our focus on U.S. imports is motivated by two facts. First, liner and air shipping are representative transport modes for U.S. imports from all but two exporting countries (e.g., Mexico and Canada). Second, previous research exploring the substitutability between air and liner shipping has mainly focused on U.S. imports (Harrigan, 2010; Hummels and Schaur, 2010, 2013). This research focused on U.S. imports because the U.S. is one of the very few countries with granular (U.S. Census) data on freight rates, quantities, and product prices by mode of transportation. Such data are essential for estimating demand-side parameters, including the elasticity of substitution between air and liner shipping.[6]

[4] According to our calculations, the average ratio of grams of CO_2 per ton of goods transported by air relative to American containership routes results in a 90-fold difference. This 90-fold difference grows to 156 if we compare grams of CO_2 per ton-mile since air routes are typically more direct than containership routes.

[5] See, for example, literature on *Gruenspecht effect*, where the impact of stricter emission regulations of new vehicles is offset by the owners keeping older vehicles for more prolonged time (Gruenspecht, 1982; Jacobsen and van Benthem, 2015).

[6] We estimate the within-route elasticity of substitution to be -7.3, where a route is defined by the country of origin and the U.S. customs District of entry.

In addition to demand-side parameters, we also need to understand what changes IMO2023 would require from the international freight shipping's supply side. IMO2023 targets *operational* efficiency, which measures actual emissions per mile-ton. Operational efficiency depends on two components: (i) *design* efficiency, determined by the technical characteristics of the vessel (e.g., its size, engine type, availability of scrubbers, etc.) and (ii) *operational* efficiency, determined by the operation mode of the vessel, including its speed. Importantly, operational efficiency can be significantly improved by slow steaming —i.e., decreasing the vessel's speed.[7] IMO members and industry practitioners stress that, at least in the short-run, slow-steaming is the best (read: only) way to achieve carbon intensity thresholds set by IMO2023 (Tirschwell, 2019; Szakonyi, 2021; Slaughter, 2022).

To quantify required supply-side changes, we evaluate vessel-specific cost and effectiveness of abatement, design, size, speed, trade routes, etc. Towards this goal, we apply standard naval engineering formulae (Corbett et al., 2009) to guide our analysis. For our supply-side analysis, we use four data sources: Clarksons World Fleet Registery (WFR), EMSA THETIS-MVR, Panjiva bill of lading data, and BlueWaterReporting. These data allow us to calculate the required speed reduction per vessel and route. In practice, we predict such reductions to be highly heterogeneous across vessel and route dimensions. On average, U.S.-bound ships will need to reduce their speed by 9.1% to meet IMO2023's efficiency standards. In the short run, slow-steaming will mechanically lead to a capacity reduction as liner shipping is a capacity-constrained industry with an average time to build a new ship of about three years.[8]

With our estimated demand- and supply-side parameters, we predict IMO2023 to have the following (short-run) effects on US-bound air and liner transportation. For the US-bound liner fleet, IMO2023 will (i) add two days to a typical route, thus reducing U.S.-bound liner capacity by 6.6%, which (ii) will lead to an increase in the average freight rate by 10% and consequently (iii) will decrease liner CO_2 emissions by 13%. For imports transported by air, we quantify the effect of IMO2023 for several scenarios, depending on the elasticity of the air freight rate with respect to vessel freight

[7] The rule of thumb from the transportation literature is that slowing down by 15% decreases emissions by 20%.
[8] See a New York Time, June 17, 2020 article by Niraj Chokshi for more details on the modern liner fleet building.

and consumers' preferences for faster delivery of goods transported by ocean containers.[9] We predict that air-transport-related CO_2 emissions will increase by up to 43%. As a result, IMO2023 will *increase* the total CO_2 emissions produced by liner fleet and air transportation by up to 28%. On top of the harms of additional CO_2 emissions, fewer goods delivered at slower speeds and higher freight rates place IMO2023's welfare losses to American consumers between 5 to 9 billion USD.

Our analysis demonstrates that when in charge of regulatory activities, specialized agencies are likely to focus only on agency-specific goals.[10] We contend that the IMO, which includes the representatives of carriers, shipbuilders, and shipping-related bankers, has proposed a reform that only aligns with sectoral interests: IMO2023 will (i) improve the image of the industry by decreasing emissions produced by (liner) maritime shipping, (ii) increase short-run profits of carriers, and (iii) will increase demand for new vessels in the medium and long run. IMO2023's double hit of likely combined transport net emissions increases and material consumer surplus reductions are outside the scope of (and are therefore irrelevant to) the IMO.

Reorganizing the remit, resources, and coordination of U.N. agencies is a complex task. However, the U.N. can charge specialized agencies with broader goals, which is likely to achieve better (read: policy consistent) outcomes. In the case of IMO2023, even if the IMO has direct influence only over vessels—if it wants—the IMO can potentially reduce combined emissions from air and liner transportation. We demonstrate this point by expanding our model to include speed as an endogenous choice of carriers. Using this model, we show that, in the case of U.S. imports, subsidizing liner carriers' fuel costs leads to lower combined (air and liner) emissions. With cheaper fuel, carriers will choose to move faster, which will immediately increase their effective capacity (while keeping the number of vessels constant) and lower freight rates. As a result, the amount of liner transportation will increase while the utilization of air transportation will decrease. Given a much higher carbon

[9] The liner-to-vessel freight rate sensitivity is difficult to estimate from the regular co-movements of these two freight rates since they are often affected by the same demand and supply factors. Another aspect of the air-transportation which complicates the analysis is that a large portion of commercial air transportation is done using the residual weight capacity of passenger airplanes.

[10] Within the UN, there are different entities considering environmental policies for liner shipping, air travel, production, etc.

intensity of air transportation, this change will *decrease* the joint emissions—according to our calculations, by up to 18%. Importantly, since the total amount of imported goods will increase, these changes will be accompanied by an *increase* in consumer surplus from imports.

Inter-sectoral leakage is also critical for academic research on emissions from transportation. For example, research on emissions from international maritime transport, while addressing in great detail spatial leakage, tends to ignore inter-sectoral leakage. Unsurprisingly, typical literature policy recommendations include either quantitative emissions restrictions or taxing bunker fuel used in ocean transportation (Parry et al., 2018; Mundaca et al., 2021). According to our results, such policies are likely to increase joint air and ocean transportation emissions, counter to the spirit of the proposed policy reform.

Our paper proceeds as follows. Section 2 provides an overview of IMO2023, our shipping microdata, and IMO2023 impacts on vessel speed and attendant short-run U.S. liner-shipping capacity removal. Section 3 provides our theoretical model. We estimate and calibrate model parameters in Section 4. In section 5, we present our quantitative predictions on the effect of IMO2023 on liner and air transportation emissions. Section 6 discusses alternative policies, such as taxing and subsidizing fuel in liner shipping. Section 7 concludes.

2 The Anatomy of IMO2023

The International Maritime Organization (IMO) is one of the U.N.'s specialized agencies tasked with devising and promulgating international freight shipping safety and environmental standards. To that end, the IMO adopted its Initial IMO Strategy on Reduction of GHG Emissions in 2018, which attempts to restrict CO_2 emissions from maritime transportation beginning in 2023[11] with more stringent measures added gradually up until 2050. We refer to all the regulations and policy changes envisioned by the IMO as IMO2023.[12] IMO2023 aims at decreasing carbon emissions by setting stricter

[11]The next round of negotiation regarding IMO2023 is set for Spring 2023 with the goal to conclude the negotiations in July 2023 (IMO, 2022).

[12]Emission threshold policies can be traced back to the Initial IMO Strategy on reduction of the GHG adopted in April 2018 (IMO Resolution MEPC.304(72)), which was later extended with new regulations adopted in 2021 (see IMO

operational efficiency standards. Operational efficiency standards are used to benchmark vessels carbon emissions in terms of the vessel's grams of CO_2 produced per tonne-mile; the IMO calls this measurement is a "Carbon Intensity Indicator (CII hereafter)." IMO2023 proposes to assign letter grades to individual ships on the basis of vessel v in year t's observed CII($CII^{obs}_{v,t}$)'s deviation from the IMO's required CII, $CII^{req}_{v,t}$. Letter grades cutoffs and the CII's formulas are provided in Table 1. Only vessels that score "A", "B", or "C" may be charted without extensive operational changes starting in 2023.

Table 1: IMO2023 Letter Grade Classification of Carbon Efficiency

$\frac{CII^{obs}_{v,t}}{CII^{req}_{v,t}} \times 100\%$	$< 83\%$	$83 - 94\%$	$94 - 107\%$	$107 - 119\%$	$> 119\%$
Grade	A	B	C	D	E

Note: $CII^{obs}_{v,t} = \frac{\text{CO}_2 \text{ Emissions}_{v,t}}{DWT_v \times Dist_{v,t}}$ and $CII^{req}_{v,t} = \left[1984 \times (DWT_v)^{-0.489}\right](1 - Z_t)$, where DWT_v—Deadweight Tonnage— is a measure of vessel size; $Dist_{v,t}$ is the total distance traveled by v in year t; expression in [.] is the reference line in year 2019; and Z_t starts out at 5% in 2023 and increments by 2% each year with the rate likely to accelerate in 2027.[13]

To determine a vessel's letter grades, we need to know vessel-specific deadweight tonnage (DWT hereafter), distance traveled, and CO_2 emissions. We get the DWT for all containerized vessels from the *World Fleet Register* (WFR), maintained by Clarksons PLC—the world's leading shipbroker. There is no comprehensive dataset on the observed CO_2 emissions at the vessel level. However, a partial dataset is provided by *THETIS-MRV* (alternatively THETIS), an online port state control/inspection database maintained by the European Maritime Safety Agency (EMSA).[14] THETIS reports observed carbon emissions (along with the distance traveled) for years 2018-2020 for 39.7% of the global liner fleet by count and 54.1% by capacity.

Using these data we (i) calculate IMO2023 letter grades for the reported by THETIS vessels (displayed in Figure 1)[15] and (ii) estimate CO_2 emissions for the remaining vessels, which allows us to calculate their letter grades. Figure 1 plots the relationship between vessel DWT and observed CO_2

Resolutions MEPC.335(76), MEPC.336(76), MEPC.337(76), MEPC.338(76)).

[14]See Online Appendix A.1 for a more detailed description of this and other datasets used in the paper.

[15]Each dot represents one of the 1903 containerized vessels for which THETIS has data on their CO_2 emissions between 2018 and 2020. In cases when there is more than one observation per vessel, they were averaged at the vessel level. The DWT data comes from Clarksons.

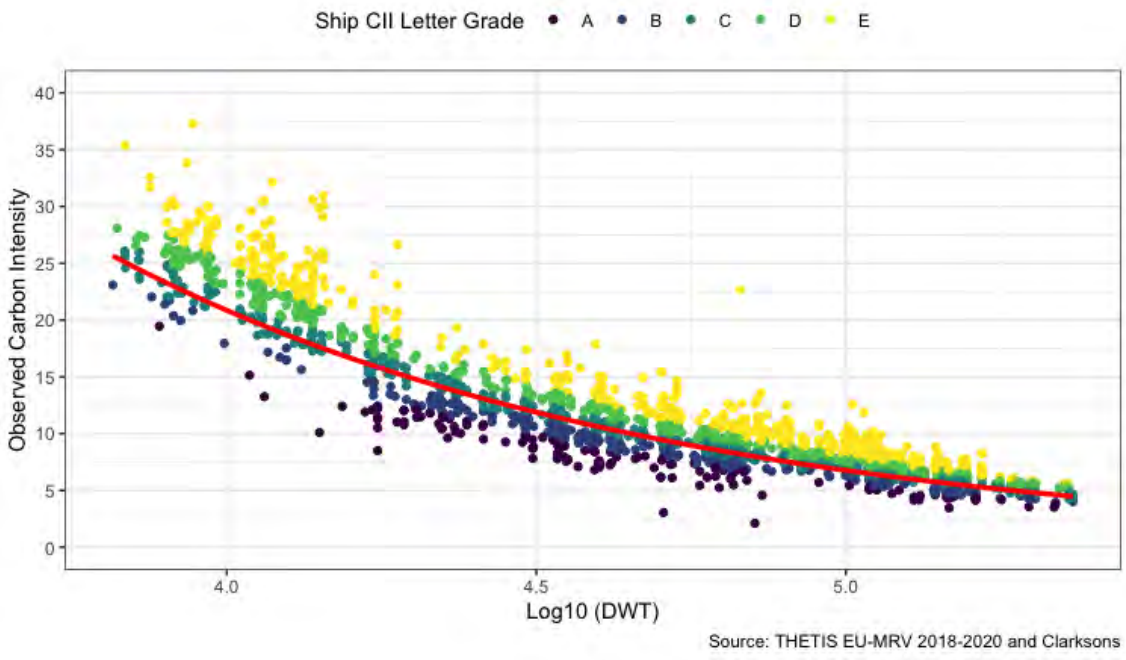

Figure 1: Observed Carbon Intensity
Note: Each dot represents a vessel. Based on DWT capacity, our sample has the following distribution of CII letter grades going based on the 2023 CII^{req} line: 5.1% are A, 12.8% are B; 25.0% are C; 27.3% are D; and, 29.8% are E.

emissions per DWT tonne-mile and includes the IM2023 CII^{req} (red) benchmark efficiency line for year 2023. Figure 1 illustrates two key insights:

- **"IMO2023 call for 5% CO_2 reduction" is an uninformative summary of potential impacts.** Industry headlines summarize IMO2023's effects as modest, citing a mere 5% reduction of vessel operational carbon intensity (Splash247.com). In practice, required CO_2 reductions will vary widely across container ships. For vessels to avoid an IMO2023 "D" or "E" rating, the average required CO_2 reduction is 8.9%. Recall that the "5%" reduction comes from $Z_{t=2023}$, which is merely a reduction relative to a 2019 IMO reference line as opposed to the vessel's observed carbon efficiency. This 8.9% average reduction reflects all vessels, including those with $A - C$ ratings. If we limit our attention to vessels that will achieve a "D" or "E" rating, then the average required reduction rises to 15.9%.

- **Vessel size is a good predictor of observed CII,** as demonstrated by a simple linear model

estimated on our THETIS sample:[16]

$$\ln\left(CII_v^{obs}\right) = \underset{(0.04)}{7.62} - \underset{(0.004)}{0.49}\ln(DWT_v) + \varepsilon_v \quad (R^2 = 0.87; \text{N Obs} = 1903) \tag{1}$$

That is, vessel size explains 87% of variation in log transformed *observed* carbon intensity.

Motivated by the high explanatory power of the DWT, we estimate the CII^{obs} for vessels outside of THETIS sample. Towards this goal, we partition our THETIS sample into a training dataset (80% of the sample) and a testing dataset (20% of the sample) 10,000 times. We fit a simple linear model in the style of equation (1) per iteration and calculate in-sample and out-of-sample R^2 and RMSE.[17] We choose our predictive model based on which model's slope term has the highest frequency across all 10,000 trials. The model's coefficient turned out to be exactly the same as in Equation 1 above. Using this model, we imputed the CII^{obs} and the letter grade classification for the remaining vessels.

2.1 Calculating the required slow-steaming in response to IMO2023

How can vessels with letter grades D and E comply with IMO2023? To date, container ship carbon abatement has come through three channels: (1) adoption of lower carbon content fuels; (2) incorporation of more fuel-efficient ship designs; and (3) construction of larger vessels. Of these channels, the first two come with more limited potential for lasting environmental improvement. Alternative fuel sources, such as liquefied natural gas and methanol, release comparable carbon emissions over their lifetime use, and vessel-design-based reductions are only realized when vessels operate at slow speeds (Winnes et al., 2015). Therefore, both IMO and practitioners emphasize slowsteaming—i.e., speed reduction—as a primary method of complying with IMO2023.[18]

[16] Standard errors are reported under coefficient estimates

[17] CII_v^{obs}, t must be expressed in levels whereas our fitted values our expressed in logs. Therefore, we exponentiate our fitted values and adjust by a Duan's smear of ≈ 1.02. Accordingly, our in-sample R^2 based on levels for our chosen model is 0.818 with a 95% CI of [0.754, 0.877]; standard errors are derived using 10,000 bootstrapped samples. More reassuringly, our out-of-sample R^2 based on levels is 0.883 with a 95% CI of [0.860,0.907].

[18] Xavier Destriau, ZIM executive vice president, stated on an August 18th, 2021 interview to Szakonyi (2021) that

> "What we [Zim] anticipate is that the first thing that will be asked of us is to reduce carbon emissions. And the only possible way emissions can be reduced is by changing the power of the engine and a ship's speed,"

To estimate the required by IMO2023 speed reduction, we first employ a naval engineering formula to express the vessel's fuel consumption F as a function of its speed (Corbett et al., 2009):

$$F_{ijv}(s_{1v}) = \left[MF_v\left(\frac{s_{1v}}{s_{0v}}\right)^3 + AF_v\right]\frac{d_{ij}}{24s_{1v}}, \tag{2}$$

where MF_v and AF_v are vessel v's main and auxiliary engine fuel consumption, respectively; s_{0v} and s_{1v} are v's design and operational speeds, respectively; and d_{ij} is the total distance of the ij route. Second, we assume that the auxiliary engine fuel consumption can be expressed in terms of the main fuel consumption:

$$AF_v s_{0v}^3 = \alpha MF_v, \tag{3}$$

and, using Clarksons data on 3,194 vessels with complete main and auxiliary engine power rating and design speed data, estimate $\widehat{\alpha} = 2963.13$ (s.e. 12.65).[19] Third, using equations (2) and (3), and by setting $\rho_v \equiv s_{1v}/s_{2v}$, we define the ratio of fuel consummations for speed s_{2v} over that for s_{1v} as

$$\frac{F_{ijv}(s_{2v})}{F_{ijv}(s_{1v})} = \left(\frac{s_{2v}^3 + \alpha}{s_{1v}^3 + \alpha}\right)\frac{s_{1v}}{s_{2v}} = \left(\frac{\rho_v^3 s_{1v}^3 + \alpha}{s_{1v}^3 + \alpha}\right)\frac{1}{\rho_v}. \tag{4}$$

For operational speeds, we use Clarksons WFR data on the vessel-specific speed.[20] As shown by Figure A3, the operational speed is highly heterogeneous and varies between 9 and 22 knots per hour: using ship capacity as weights, containerships on average travel at 15.2 knots per hour. Equation 4 allows us to calculate the required proportional decrease in speed of vessels currently classified below grade C to achieve the minimum required threshold for grade C, which, as defined by Table 1, is equal to $\frac{CII_{v,t}^{obs}}{CII_{v,t}^{req}} = 1.07$.

Based on this threshold and equation 4, we numerically solve for ρ_v for each of the vessels which

he said. That means the industry is going "to need more vessels to handle the same amount of cargo."

Garret Bowman, President of Gulfstream Shippers Association stated that "I think we'll see a lot of ships slow down [in response to IMO2023]" (Slaughter, 2022).

[19] We used weighted OLS without the intercept term with vessel TEU as weights. The R^2 is 0.83.

[20] Clarksons maintains its own vessel tracking AIS service, SeaNet. Clarksons uses SeaNet travel time estimates when it puts its WFR dataset together.

are classified with a grade of D or E, while setting $\rho_v = 1$ for all other vessels (i.e., classified as A-C).[21]

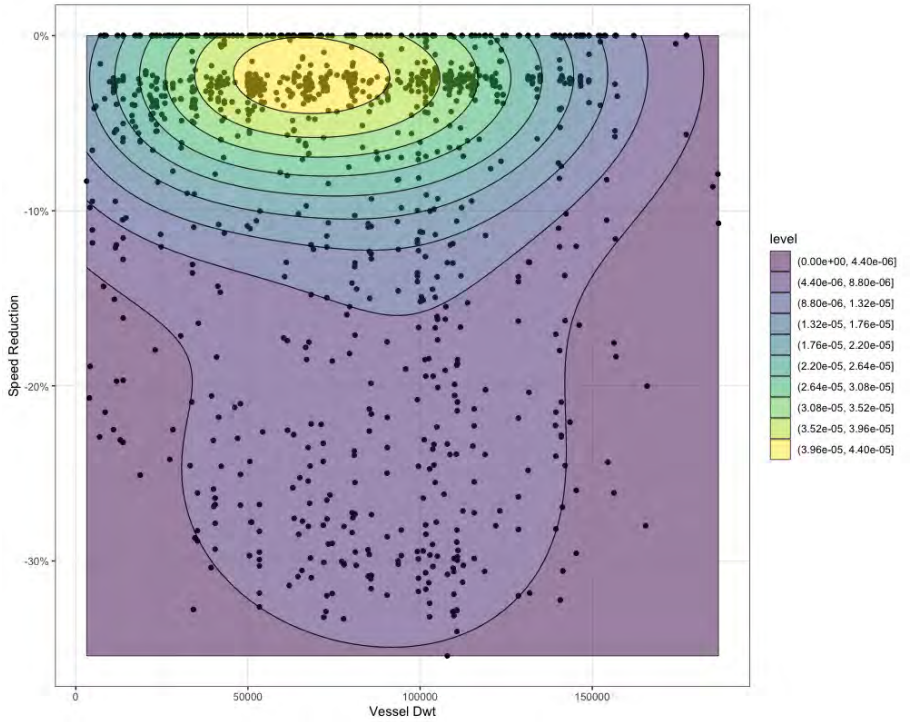

Figure 2: Speed Reduction

Figure 2 presents our estimates of $(\rho_v - 1) \times 100\%$ plotted against the DWT; vessels with grades A-C are depicted by dots on the 0% horizontal axis. Different colors provide information about the density by count (e.g., how many ships are both 10,000 Dwt and need to slow down 10%), with the contour lines marking out the boundaries between different discrete intervals. From the Figure, many vessels, especially the smaller- and medium-size ones, need to slow down. On a capacity-weighted average, U.S.-bound ships need to reduce speed by about 6.4% to meet IMO2023 standards, increasing the average shipment time by 1.9 days per route.

[21] While Equation (4) admits a closed form solution for ρ_v, this solution is cumbersome enough for the numerical solution to be more expedient while remaining accurate. For vessels requiring a speed adjustment, we proceed accordingly. Suppose $\frac{CII_v^{obs}}{CII_v^{req}} = x \geq 1.07$. This would imply that vessel v would need to improve its operational CO_2 efficiency by $x - 1.07$; equivalently, v could reduce its fuel consumption via slow steaming such that ratio of its fuel consumption post-slow down relative to pre-slowdown equals $1 - (x - 1.07)$. Thus, we find the slow down adjustment ρ_v by setting $H(\rho_v) = 0$ such that $H(\rho_v) \equiv \left(\frac{\rho_v^3 s_{1v}^3 + \alpha}{s_{1v}^3 + \alpha}\right)\frac{1}{\rho_v} - \left(1 - (\frac{CII_v^{obs}}{CII_v^{req}} - 1.07)\right)$.

2.2 Calculating effective capacity reduction

In this section, we will demonstrate that since (i) liner shipping operates at full capacity and (ii) building new vessels requires years, in the short run, slowsteaming lowers liner fleet capacity. To evaluate the level of the utilized capacity by the liner fleet, we use Clarksons Shipping Intelligence Network (SIN). Specifically, using SIN, we calculate the idle TEU capacity of the liner fleet between 2014 and 2022 at the daily frequency and plot it in Figure 3. Figure 3 illustrates that on any given day in this time period, the idle capacity varies between 1.3% and 6.8%. On average, the idle TEU capacity is between 2 and 3%. While in some cases, idle capacity comes from a lack of demand (e.g., Spring and Summer of 2020 due to the outburst of COVID), idle capacity is frequently a function of port congestion. For example, Shippingwatch.com, Sep 24, 2021 blamed port bottlenecks for the long waiting times outside the ports with the most extended wait of up to 22 days. Furthermore, in some cases, it can result from maintenance and adjusting to the rotation schedule. Therefore, we consider the observed idle rates to be consistent with the full employment of the liner fleet.

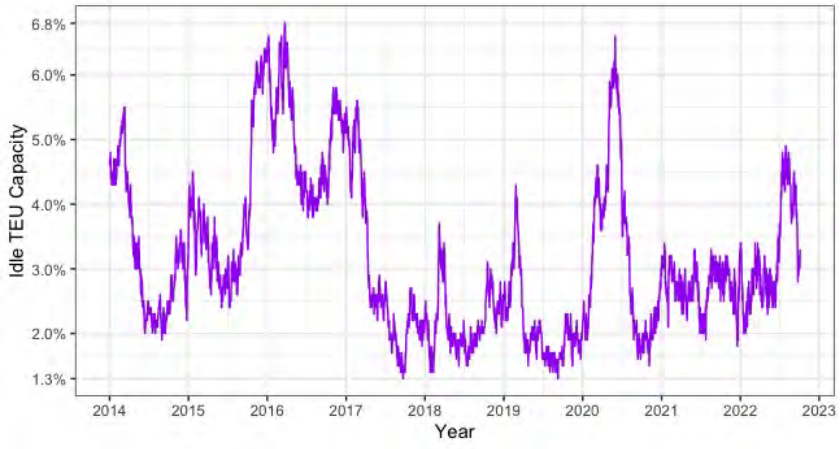

Figure 3: Historic Daily Idle Liner TEU Capacity
Sources: Figure 3 relies on data from Clarksons Shipping Intelligence Network (SIN).

In the short run, liner shipping is capacity constrained as it requires up to three (3) years to build a new vessel.[22] Therefore, the required slow-down of the liner fleet, analyzed above, will effectively reduce the liner fleet capacity. To quantify this effect, we use calculated vessel speed reduction ρ_v to

[22]See a New York Time, June 17, 2020 article by Niraj Chokshi for more details on the modern liner fleet building.

determine the reduced number of round trips a vessel can make during the year. A vessel's capacity is the product of its TEU capacity and the number of annual round trips. The number of round trips for vessel v on route n_{ijv} is given by

$$\text{Round Trips} : n_{ijv} = A \Big/ 2(TIME_{ij} + \text{port time}(TEU_v)), \tag{5}$$

where A is the number of sailing days in the year and $TIME_{ij}$ is the average route time of the vessel.[23] We estimate port time in hours as a function of vessel TEU capacity using CMA-CGM (the world's 3rd largest carrier) publicly posted data for American ports.[24] Our simple regression model is:[25]

$$\ln(\text{port time}_v) = \underset{(0.33)}{-2.49} + \underset{(0.04)}{0.67} \ln(TEU_v) + \varepsilon_v \quad (R^2 = 0.30; \text{N Obs} = 744). \tag{6}$$

Given that the annual ship capacity is $TEU_v \times n_{ijv}$, we sum up over all ships in a given route ij to yield the route's annual capacity. Armed with the new (read: smaller) number of round trips $n_{ijv}^{\text{Post}}(\rho_v)$, we compute the reduction of post-IMO2023 route capacity to pre-IMO2023 capacity as:[26]

$$\underline{\omega}_j = 1 - \frac{\sum_{i,v \in V_{ij}} n_{ijv}^{\text{Post}}(\rho_v) TEU_v}{\sum_{i,v \in V_{ij}} n_{ijv}^{\text{Pre}} TEU_v}, \tag{7}$$

where V_{ij} is the set of all containerships serving route ij. The slow down analogue of capacity reduction $\underline{\omega}_j$ is likewise given by:

$$\underline{\rho}_j = \frac{\sum_{i,v \in V_{ij}} \rho_v TEU_v}{\sum_{i,v \in V_{ij}} TEU_v} \leq 1. \tag{8}$$

[23] We assume that vessels are active for A =340 days out of the year to reflect off-hire periods or when statutory maintenance, dry docking, etc. occurs Haralambides (2019).

[24] CMA-CGM lists vessel names but not vessel IMO numbers. We use Vessel Tracking to match CMA-CGM vessels to IMO numbers. Once we have IMO numbers, we can retrieve vessel TEU capacity from our Clarksons data.

[25] Since we need estimates of port time in hours, not log hours, we need to transform this model back to levels. The Duan smear for model (6) is 1.273719.

[26] We use BlueWater Reporting data on to measure both route ij's distance and time at sea (e.g., $TIME_{ij}$). We use BlueWater's 2019 rotation information to calculate pre-reform speed, namely $TIME_{ij}^{\text{Pre}}$. See Online Appendix A.2 for more information on how we construct routes ij and compute voyage time.

When we apply $\underline{\omega}_j$ to pre-slowdown volumes, we calculate that IMO2023 will translate into a 6.57% capacity reduction. However, this aggregate reduction obscures heterogeneity across countries' capacity reduction. Figure 4 presents calculated $\underline{\omega}_j$'s across exporters to the U.S. For example, Chinese liner export capacity should fall by about 5.60%, French—by 9.02%, and Georgian—by over 15%.

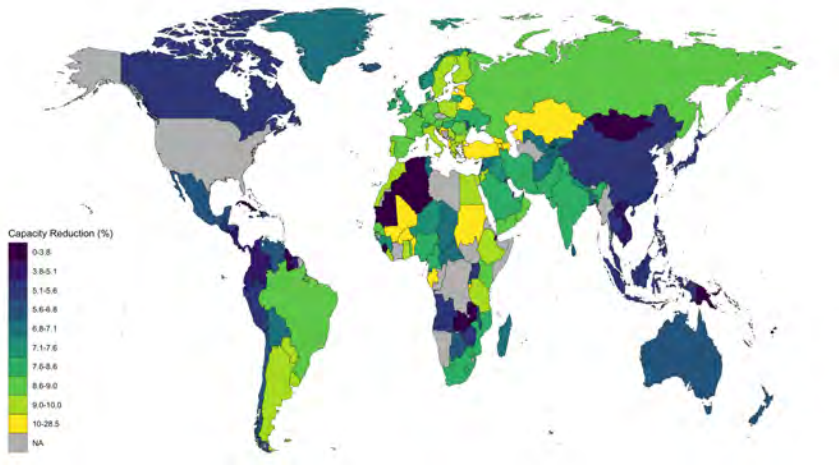

Figure 4: IMO2023 US Capacity Impacts

Enforcement Mechanism. As with previous IMO regulatory efforts, enforcement is generally left to member states. Once recommendations made by the IMO's Marine Environment Protection Committee (MEPC) are amended to the MARPOL convention[27] implementation details are often left to MARPOL signatories. To take the U.S. as an example, MARPOL Annex IV "Regulations for the Prevention of Air Pollution from Ships", has been incorporated into U.S. law by the Act to Prevent Pollution from Ships (APPS) and implemented within 33 USC 1901 and 33 CFR 151" (USCG, 2022). When it comes to the regulation of the sulfur content in bunker fuels used by commercial vessels (part of Annex IV), Hansen-Lewis and Marcus (2022) cite the U.S. Coast as one such enforcement entity of maritime emissions standards.

Proponents of the IMO's role in improving maritime emissions through cooperation with port states (read: MARPOL signatories) point to the success of "IMO2020." IMO2020 was a rule change

[27]MARPOL stands for "International Convention for the Prevention of Pollution from Ships, 1973 as modified by the Protocol of 1978" and is one of the world's most significant international marine environmental conventions; see the U.S. Coast Guard's summary page here.

that lowered the maximum sulfur content in the fuel used by vessels outside of emission control areas to 0.50% m/m (mass by mass)- a large drop from the previous 3.5% m/m standard. Yuan et al. (2022) find using satellite imagery that, even controlling for the reduction of commercial freight traffic due to COVID-19, the IMO2020 was a success on its own terms, with 46% reduction of SO_2 aerosol volume. Unfortunately, the enforcement mechanism remains confusing for owners and charters and thus may potentially delay the implementation of IMO2023 (Kinyua, 2023).

3 Model

Our model builds on the previous work by Hummels et al. (2009) and Hummels and Schaur (2013) on international transportation. The model is set from the perspective of one country, Home, which consists of multiple regions indexed by i and imports foreign goods using two modes of transportation: liner and air shipping. Our key assumptions are:

(A1) **Substitutability between imports delivered by air and liner shipping.** Hummels and Schaur (2013) demonstrated this substitutability for goods even within narrowly defined HS10 product categories. The substitutability across different types of products is consistent with the theoretical frameworks of Krugman (1980) and Melitz (2003) and has been confirmed by the literature on estimating the elasticity of substitution across products (also refereed to as trade elasticity).[28]

(A2) **Liner shipping operating at full capacity**—as discussed in Section 2.2.

(A3) **Significant excess capacity in air shipping**—as demonstrated by previous research and our calculations. Besedeš and Murshidb (2022) argued, that, on average, only 24.3% of payload is used to ferry cargo. Using Domestic and International Segment T100 Traffic Data, we confirm this statement and plot the utilized air capacity over time and across airplane types in Figure 5. Similar to Besedeš and Murshidb (2022), we find that most of the under-utilized capacity comes from the passenger airplanes, which are responsible for 44% of cargo transported by air (Budd and Ison, 2017).

[28] See, among others, Soderbery (2015); Lashkaripour and Lugovskyy (2022). This substitutability will ensure that, if the delivered price of vessel-shipped goods (e.g., cars) increases, the quantity of the air-shipped goods (e.g., cell phones) increases.

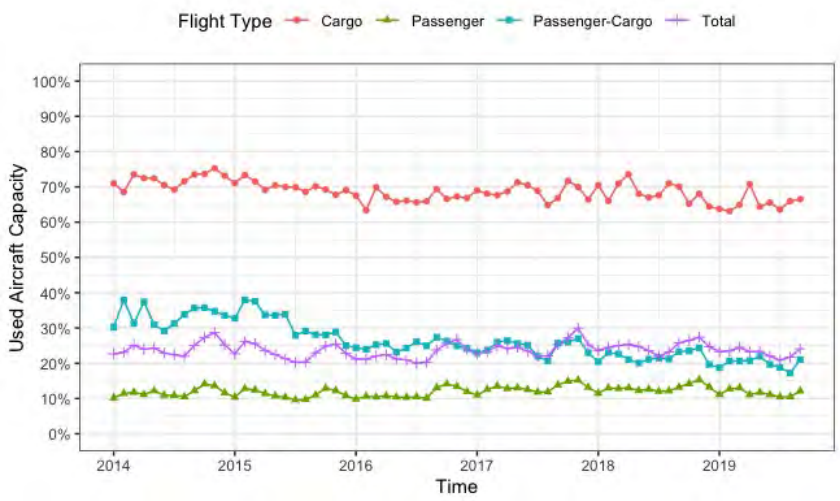

Figure 5: US Air Import Capacity Utilization over Time
Sources: Figure 5 relies on Domestic and International Segment T100 Traffic Data reported by U.S. and Foreign Carriers and provided by the Bureau of Transportation Statistics (BTS).

(A4) **Route Stability.** In our quantitative analysis, we assume that routes connecting exporting countries and Home's regions are unaffected by the considered policies. This assumption is consistent with the conclusions of Heiland et al. (2022), who found that "the shipping network is stable over time" even when comparing pre and post Panama Canal expansion in 2016. Furthermore, we provide our analysis in Online Appendix A.4 showing that routes remained quite stable between 2013 and 2020 despite significant variation in fuel prices during the same period.[29]

(A5) **Ignoring Several Freight Rate Determinants.** To preserve the tractability of our model, we abstract away from several very important issues that affect the formation of freight rates, such as port efficiency (Blonigen and Wilson, 2008), the number of carriers and trade volumes (Hummels et al., 2009; Ardelean and Lugovskyy, 2023) average vessel size (Asturias, 2019), average unit values (Hummels and Skiba, 2004), geography and networks in liner shipping (Ganapati et al., 2020), and backhaul effects (Ishikawa and Tarui, 2018; Wong, 2020).[30]

[29] See, for example, EIA for oil price trends.

[30] In the estimation part, we justify this assumption on the basis that these determinants are already embedded in the observed freight rates. When analyzing policy-induced changes, we will implicitly assume that even if a policy affects some of these determinants (e.g., trade volumes), these changes will have a second-order effect on the freight rates compared to the policy's direct effect.

3.1 Benchmark Model

Preferences. Consumers have Cobb-Douglas preferences defined over a domestically-produced composite good 0 and composite differentiated good. Differentiation is based on the national origin [31] j and goods' perishability: perishable vs. non-perishable. We use the lower-bar and upper-bar notation for quantities, prices, and other parameters of non-perishables and perishables, respectively. Formally, a Home's representative consumer in region i in year t has preferences given by:

$$U_{it} = q_{0,it}^{1-\mu}\left[\sum_j \left(\kappa_{it}\kappa_j \underline{q}_{ijt}^{\frac{\varepsilon-1}{\varepsilon}} + \overline{q}_{ijt}^{\frac{\varepsilon-1}{\varepsilon}}\right)\right]^{\mu\frac{\varepsilon}{\varepsilon-1}} \qquad \varepsilon > 1, 1 > \mu > 0, \tag{9}$$

where $\underline{q}_{0,it}$ is the quantity of the domestic numeraire good;

$\underline{q}_{ijt}$ and $\overline{q}_{ijt}$ are the imported from j quantities of non-perishables and perishables, respectively;

κ_{it} and κ_j are the region-time- and origin-specific preference shifters of non-perishable imports;

Supply Side and Transportation. Production costs may vary across countries of origin, over time, and between perishable and non-perishable goods. Prices, freight rates, and tariffs are set exogenously. Perishable goods are imported by air, while non-perishables—by ocean. We assume that the air freight rate is always much greater for air than for ocean: $\overline{f}_{ijt} >> \underline{f}_{ijt}$, and therefore firms choose to transport non-perishable goods by vessel. Following Hummels et al. (2009), we express the delivered prices of imported goods imported by i from j in t, and denoted by P_{ijt}, as a function of the free-on-board (FOB) prices, p_{ijt}, iceberg tariffs, $\tau_{ijt} \geq 1$, and specific transport cost, f_{ijt}:

$$\underline{P}_{ijt} = \underline{p}_{ijt}(\underline{\tau}_{ijt} + \underline{f}_{ijt}/\underline{p}_{ijt}), \qquad \overline{P}_{ijt} = \overline{p}_{ijt}(\overline{\tau}_{ijt} + \overline{f}_{ijt}/\overline{p}_{ijt}). \tag{10}$$

[31] The national origin, or Armington, differentiation is quite common in trade literature and has also been used in the related paper on emissions from transportation of traded goods by Shapiro (2016).

Equilibrium Import Demand Functions. In equilibrium, the ratio of marginal utilities is equal to the ratio of the delivered prices, from which we can derive demand functions:

$$\underline{q}_{ijt} = \left(\kappa_{it}\kappa_j q_{0,it}\right)^{\varepsilon}\left(K_{it}\underline{p}_{ijt}(\underline{\tau}_{ijt} + \underline{f}_{ijt}/\underline{p}_{ijt})\right)^{-\varepsilon}, \qquad \overline{q}_{ijt} = \left(q_{0,it}\right)^{\varepsilon}\left(K_{it}\overline{p}_{ijt}(\overline{\tau}_{ijt} + \overline{f}_{ijt}/\overline{p}_{ijt})\right)^{-\varepsilon}, \tag{11}$$

where $K_{it} = \frac{1-\mu}{\mu}\left[\sum_j\left(\kappa_{it}\kappa_j\underline{q}_{ijt}^{\frac{\varepsilon-1}{\varepsilon}} + \overline{q}_{ijt}^{\frac{\varepsilon-1}{\varepsilon}}\right)\right]$ is treated by all market participants as given. Notably, the demand for any differentiated variety depends on the freight rates of all other imported varieties delivered to district i.

3.2 Extended Model with the Endogenous Speed of Ocean Carriers

In the extended model, we consider profit-maximizing liner carriers, which choose both their speed and freight rate. Our modeling exercise provides a disciplined approach to predicting changes in carrier behavior in response to exogenous policy shocks. Using engineering formulas of fuel consumption as a function of speed, we model the profit-maximizing behavior of carriers, which select their speed based on (i) fuel cost and (ii) consumers' preferences for faster delivery. In the process, we allow for scale effects based on the vessel size and distance traveled.

Route Fuel Costs. From eq. (2), the fuel consumption of vessel v, F_v, is a function of fuel consumption by main and auxiliary engines (MF_v, AF_v), speed s, and distance d : $F_v = \left(MF_v\left(\frac{s_v}{s_{0,v}}\right)^3 + AF_v\right)\frac{d}{24s}$. To enable a quantitative evaluation of our model, we assume that route ij is served by a representative carrier with a vessel size TEU_{ij}.[32] With that in mind, we express the annual fuel cost on route ij as:

$$\underline{C}_{ij}(s_{ij}) = \left[\underbrace{n_{ij}(s_{ij})}_{\text{total number of trips}} \times \underbrace{b}_{\text{fuel price}} \times \underbrace{F_{ij}(s_{ij}; TEU_{ij}, d_{ij})}_{\text{fuel consumption per trip}}\right]^{\phi}, \tag{12}$$

where the number of trips $n_{ij}(s_{ij})$ for a given speed s_{ij} and vessel size TEU_{ij} comes from eq. (5), fuel consumption per trip from eq. (2), and ϕ captures potential curvature of the cost function.

[32] As we show in Section 4.3, vessel size can be used to approximate remaining technical characteristics.

This curvature comes from the fact that, in reality, route ij can be served by a mix of heterogeneous vessels with different fuel consumption per TEU. Specifically, larger vessels have a much lower fuel consumption per mile-TEU than smaller vessels. Thus, routes with a heterogeneous mix of vessels (potentially busier routes) may experience significant deviations in the average fuel consumption compared to the benchmark case of a route being served by a representative vessel type.

Route Volume. Let x_{ij} be the TEU equivalent of the annual quantity of goods shipped by containers on a given route ij : $x_{ij} \equiv \gamma^{\text{TEU}} \underline{q}_{ij}$.[33] Ignoring the divisibility porblem, x_{ij} is equal to the number of round trips $n_{ij}(s_{ij})$ times the TEU capacity of the representative carrier TEU_{ij}. In this way:

$$\underline{q}_{ij} = \frac{x_{ij}}{\gamma^{\text{TEU}}} = \frac{TEU_{ij}}{\gamma^{\text{TEU}}} \times n_{ij}(s_{ij}) = \frac{TEU_{ij}}{\gamma^{\text{TEU}}} \times \frac{A}{2\big((d_{ij}/24s_{ij}) + port_{ij}\big)}. \tag{13}$$

Equation (13) demonstrates that as speed increases, route volume increases.

Freight Rates. We re-arrange terms from our optimal demand function in eq. (11) to express per unit freight rate in liner shipping, $\underline{f}_{ij}$ as:

$$\underline{f}_{ij}(s_{ij}) = \underline{q}_{ij}(s_{ij})^{-\frac{1}{\varepsilon}} \frac{q_{0,it}\kappa_{ij}(s_{ij})}{K_{it}} - \underline{p}_{ij}\underline{\tau}_{ij}, \tag{14}$$

where we use the formula for $\underline{q}_{ij}$ given by (13). Freight rates depend on speed through two (2) channels: (i) through the cost of shipping as $\underline{f}_{ij}(s_{ij}) = \underline{C}_{ij}(s_{ij})/q_{ij}$ and (ii) through the preferences for timely delivery $(\kappa_{it}\kappa_j)$. We formalize the latter with the following functional form:

$$\kappa_{ij}(s_{ijt}) \equiv \kappa_{it} \times \kappa_j = \vartheta_{jt}(d_{ij}/(24s_{ij}))^{\beta_k} \qquad \beta_k < 0. \tag{15}$$

From this equation, $\kappa(s_{ijt})$ increases in the vessel's speed. As we will show next, these two counter-acting channels ($\frac{\partial \underline{f}_{ij}}{\partial \underline{q}_{ij}} < 0$ and $\frac{\partial \underline{f}_{ij}}{\partial \kappa_{ij}} > 0$) are essential in determining profit-maximizing freight rates.

[33] γ^{TEU} is the average per-unit volume of the containerized goods. We set $\gamma^{\text{TEU}} = 13.9$ tonnes per TEU. We get it by summing up the total weight of all Panjiva U.S. imports shipments in 2019 with TEU volume > 0 and then dividing it by the total number of TEU containers.

Carrier's Revenue and Profit. Multiplying route freight rates by volume yields route revenue:

$$\begin{aligned}\underline{R}_{ij}(s_{ij}) &= \underline{q}_{ij}(s_{ij}) \times \underline{f}_{ij}(s_{ij}) \\ &= n_{ij}(s_{ij}) \frac{TEU_{ij}}{\gamma^{\text{TEU}}} \left(\left[n_{ij}(s_{ij}) \frac{TEU_{ij}}{\gamma^{\text{TEU}}} \right]^{-\frac{1}{\varepsilon}} \frac{q_{0,it} \left(\theta_{it} (d_{ij}/(24 s_{ij}))^{\beta_k} \right)}{K_{it}} - \underline{p}_{ij} \tau_{ij} \right). \end{aligned} \tag{16}$$

The profit function is given by $\underline{\pi}_{ij}(s_{ij}) = \underline{R}_{ij}(s_{ij}) - \underline{C}_{ij}(s_{ij})$. This profit-maximzing speed s^*_{ij} must satisfy $\frac{\partial \pi_{ij}}{\partial s_{ij}} \equiv 0 \iff \frac{\partial \underline{R}_{ij}}{\partial s_{ij}} = \frac{\partial \underline{C}_{ij}}{\partial s_{ij}}$, which, in turn, can be written as:

$$\underbrace{\frac{\partial \underline{q}_{ij}}{\partial s_{ij}} \underline{f}_{ij} + \underline{q}_{ij} \left(\frac{\partial \underline{f}_{ij}}{\partial \underline{q}_{ij}} \frac{\partial \underline{q}_{ij}}{\partial s_{ij}} + \frac{\partial \underline{f}_{ij}}{\partial \kappa_{ij}} \frac{\partial \kappa_{ij}}{\partial s_{ij}} \right)}_{\partial R_{ij}/\partial s_{ij}} = \underbrace{\phi \Big(b n_{ij}(s_{ij}) F_{ij}(s_{ij}) \Big)^{\phi - 1} b \left(\frac{\partial n_{ij}}{\partial s_{ij}} F_{ij}(s_{ij}) + n_{ij}(s_{ij}) \frac{\partial F_{ij}}{\partial s_{ij}} \right)}_{\partial C_{ij}/\partial s_{ij}}. \tag{17}$$

This equation will be the basis for evaluating the optimal choice of speed in response to policy shocks and related changes in bunker fuel costs.

4 Estimating and Calibrating Model Parameters

In this section, we structurally estimate and calibrate model parameters which we will then use to evaluate the effects of IMO2023. We will restrict our attention to imports by the U.S. There are two reasons for this choice. First, detailed data on the import prices and freight rates by the mode of transportation is rather limited for other countries. Second, the U.S. ideally fits our model with only two modes of transportation: air and ocean, as there are only two countries, Canada, and Mexico, which use land transportation for exporting to the U.S.

4.1 Data Sources

For the demand estimation, we use monthly U.S. Census import data from 2013-2019. These data are freight-mode specific (e.g., ocean containerized, ocean non-containerized, air), are reported at the HS6 level of dis-aggregation, and specify the U.S. Custom District of entry and the exporting country.

We limit our attention to two freight import modes: ocean containerized and air. Within these data, we observe freight charges (USD), import values (USD), and import weight (kg).

Our first aggregation step is to build up mode-route-time-HS6 values for freight charges, import values, and import weight from these Census data. Next, we obtain annual-country-HS6 level U.S. import tariff data from the WITS. We use these tariff data alongside our mode-product import data to compute mode-route-time tariffs (e.g., $\underline{\tau}_{ijt}$ or $\overline{\tau}_{ijt}$) using HS6 import mode-route-time-HS6 value shares as part of this weighted average. Finally, we sum over HS6 product codes for our freight charges, import values, and import weight to arrive at the import *mode-route-time* data we use for estimation. Moreover, we aggregate our import data to quarterly time frequency. We define factory prices (p_{ijt}) as the ratio of import values to import weight, unit freight charges (f_{ijt}) as the ratio of freight charges to import weight, and ad-valorem freight costs (f_{ijt}/p_{ijt}) as the ratio of unit freight charges to factory prices.

4.2 Estimating Demand Parameters in the Benchmark Model

We start by estimating the key parameters of our model by using our theoretical relative demand equation (11). We log-linearize it: $\ln\left(\frac{q_{ijt}}{\overline{q}_{ijt}}\right) = \varepsilon\ln(\kappa_j) + \varepsilon\ln(\kappa_{it}) - \varepsilon\ln\left(\frac{\underline{p}_{ijt}}{\overline{p}_{ijt}}\right) - \varepsilon\ln\left(\frac{\underline{\tau}_{ijt}+\underline{f}_{jt}/\underline{p}_{ijt}}{\overline{\tau}_{ijt}+\overline{f}_{ijt}/\overline{p}_{ijt}}\right)$, and set our estimating equation as following:

$$\ln\left(\frac{q_{ijt}}{\overline{q}_{ijt}}\right) = \theta_j + \theta_{it} + \beta_1\ln\left(\frac{\underline{p}_{ijt}}{\overline{p}_{ijt}}\right) + \beta_2\ln\left(\frac{\underline{\tau}_{ijt}+\underline{f}_{ijt}/\underline{p}_{ijt}}{\overline{\tau}_{ijt}+\overline{f}_{ijt}/\overline{p}_{ijt}}\right) + \mu_{ijt}, \tag{18}$$

where θ_j and θ_{it} are exporter and district-year fixed effects, respectively; and μ_{ijt} is the error term. Eq. (18) has strong similarities with the estimation equation (9) of Hummels and Schaur (2013).[34] In addition to addressing multiple potential concerns with this specification,[35] they provided a detailed and convincing argument for why to identify the elasticity ε from the relative trade cost coefficient

[34]Their LHS is in terms of relative revenues rather than relative quantities. When we re-ran our eq. (18) with the relative revenues as the LHS. The only change is in the relative price coefficient, β_1 : its magnitude has increased by 1.

[35]E.g., trade costs endogeneity, unobserved (quality) terms correlated with prices, etc.

β_2 rather than from the relative price coefficient β_1.[36] Following their approach, we identify $\widehat{\varepsilon} = -\widehat{\beta}_2$. Next, we will recover κ_j by $\widehat{\kappa}_j = \exp\left(\widehat{\theta}_j/(-\widehat{\beta}_2)\right)$ and κ_{it} by $\widehat{\kappa}_{it} = \exp\left(\widehat{\theta}_{it}/(-\widehat{\beta}_2)\right)$.

Instruments. Following Hummels and Skiba (2004) and Bellemare et al. (2017), we instrument for $\ln \frac{p_{ijt}}{\overline{p}_{ijt}}$ and $\ln \frac{\tau_{ijt}+f_{ijt}/p_{ijt}}{\overline{\tau}_{ijt}+\overline{f}_{ijt}/\overline{p}_{ijt}})$ with their one-quartered lags.

Results. Table 2 presents estimation results of eq. (18). The elasticity of substitution $\hat{\varepsilon}$ is 7.3 for OLS and 10.3 for IV, respectively. Both estimates are statistically significant at 1% level. The estimates of the fixed effect θ_j and θ_{it} allow us to get the estimates of $\hat{\kappa}'$s.

Table 2: Equation (18) Results

	(1:OLS)	(2:IV)
$\ln\left(\underline{p}_{ijt}/\overline{p}_{ijt}\right)$	-0.806^{***}	-0.823^{***}
	(0.026)	(0.057)
$\ln\left(\frac{\tau_{ijt}+\underline{f}_{ijt}/\underline{p}_{ijt}}{\overline{\tau}_{ijt}+\overline{f}_{ijt}/\overline{p}_{ijt}}\right), (-\widehat{\varepsilon})$	-7.298^{***}	-10.299^{***}
	(0.561)	(2.181)
Num. obs.	22,432	18,228
Num. groups: θ_j	214	210
Num. groups: θ_{ij}	262	210
R^2 (full model)	0.583	0.588
R^2 (proj model)	0.230	0.209

$^{***}p < 0.01$; $^{**}p < 0.05$; $^{*}p < 0.1$

4.3 Estimating and Calibrating Parameters in the Extended Model

Recall that in the extended model, we allow liner carriers' freight rate and speed to be endogenously determined. Among other factors, these variables will be determined by the preferences for timely delivery (of non-perishables) β_k previously defined by eq. (15). To estimate β_k, we utilize annualized 2012-2019 BlueWater data on the average number of days in transit for every route ij, which we label as $TIME_{ijt}$. Using these data, we log-linearize eq. (15) and regress κ's on $TIME_{ijt}$ including

[36] The reason is that consumers care about the units of the goods rather than their weight, while our measure of prices is in terms of weight. Then, since the weight per unit of the air- and ocean-transported commodities is likely to differ, the coefficient on the relative prices (in terms of weight) is likely to be biased.

region-year fixed effects:

$$\ln(\kappa_j \kappa_{it}) = \beta_k \ln TIME_{ijt} + \ln(\vartheta_{jt}) + \epsilon_{ijt}.$$

Table 3 presents the results. An intuitive interpretation of this estimate is that for a given U.S. region i, a 10% increase in travel time is associated with a $\beta_k \times 10\%$ change in the preference parameters for non-perishables. In practice, this marginal effect translates into a 0.3 to 0.41% decrease.

Table 3: Preferences for timely delivery

	(1:OLS)	(2:IV)
$\ln TIME_{ijt}$, $(\widehat{\beta}_k)$	-0.041^{***}	-0.030^{***}
	(0.011)	(0.009)
Num. obs.	3806	3366
Num. groups: $\ln(\vartheta_{jt})$	608	534
R^2	0.370	0.368

$^{***}p < 0.01$; $^{**}p < 0.05$; $^{*}p < 0.1$

Turning to the cost side of the model, we first show that fuel consumption and design speed are functions of the vessel size. Towards this goal, we use data from Clarksons WFR, which allows us to match vessel size expressed in TEUs with engines' main and auxiliary fuel consumption and design speed $(s_{0,v})$. We use the following specification:

$$\log(x_v) = \alpha_1 + \alpha_2 \log(TEU_v) + \epsilon_v,$$

where x_v sequentially represents MF_v, AF_v, and $s_{0,v}$. We apply a Seemingly Unrelated Regression (SUR) estimator to simultaneously estimate all coefficients. Table 4 presents the results. Our results are consistent with the prior literature (Cullinane and Khanna, 1999) in demonstrating that fuel consumption of both engine types increases less than proportionally with the vessel size and that the design speed increases with the vessel size.

Table 4: Vessel Size as a predictor of Fuel Consumption and Speed

Dependent Variable	$\log(MF_v)$	$\log(AF_v)$	$\log(s^3_{0,v})$
(Intercept)	-2.340^{***}	-3.151^{***}	7.003^{***}
	(0.038)	(0.137)	(0.371)
$\log(TEU_v)$	0.851^{***}	0.590^{***}	0.288^{***}
	(0.005)	(0.371)	(0.044)
R^2	0.877	0.490	0.431
Num. obs.	4046	329	370
Duan Smear	1.037	1.078	1.034

$^{***}p < 0.01$; $^{**}p < 0.05$; $^{*}p < 0.1$

Calibrating scale parameter (ϕ) of carriers' cost function. In our model (eq. 12), we allow for scale effects in the carrier cost function via a scale parameter denoted by ϕ. Eq. (17) formalizes the equality of the carrier's marginal revenue and marginal cost in our model. We will use this condition to uncover ϕ and profit-maximizing speed in a two-step process so that the calibration of both parameters is internally consistent.

Step I. For a given ϕ, define optimal route ij speed as $s^*_{ij} = \zeta_{ij} s^{\mathrm{D}}_{ij}$, where s^{D}_{ij} is the average speed of the representative vessel on route ij (based on BlueWater rotation data in 2019) and ζ_{ij} is the required speed adjustment parameter. Using equation (17), recover ζ_{ij} for each route ij as:

$$\zeta^*_{ij} \in \operatorname{argmin} e(\zeta_{ij}, \phi) \equiv \Big(\partial R_{ij}/\partial s_{ij}(\zeta_{ij}) - \partial C_{ij}/\partial s_{ij}(\zeta_{ij}, \phi)\Big)^2,$$

where $e(\zeta_{ij}, \phi)$ is the squared difference between route ij's marginal revenue and cost at speed s_{ij}.[37]

Step II. Find the optimal value of ϕ by minimizing a sum of squared errors as formulated by our marginal profit condition:

$$\phi^* \in \operatorname{argmin} \sum_{ij} e\big(\zeta_{ij}(\phi), \phi\big).$$

For these steps, we use 2019 data. We do it for two reasons: (i) it is the year we use for our

[37] Since our marginal profit eq. (17) does not admit a closed form solution for s^*_{ij}, we use a simple implementation of the Brents method to solve for ζ_{ij}.

counterfactual analyses, and (ii) it provides the greatest coverage of speed/vessel data throughout our sample. We set all routes' bunker prices to be $b = 432.30$ USD/tonne based on a simple average of 2019 bunker data made available via Clarkson's SIN data service. Lastly, since our marginal profit condition depends on whether or not our preference shifter κ is a function of speed, we have two calibration settings for ϕ^*: one where $\frac{\partial \kappa}{\partial s_{ij}} = -\beta_k \vartheta_{jt} (d_{ij}/(24 s_{ij}))^{\beta_k - 1} \frac{d_{ij}}{12 s_{ij}^2} \neq 0$ and the other where $\frac{\partial \kappa}{\partial s_{ij}} = 0$.

We report both the OLS and IV estimates of the curvature parameter $\phi*$ in Table 5: They range between 1.12 and 1.18 and are statistically significant. The fact that the estimates of $\phi*$ are greater than one confirm our prior that busier routes (which are more likely to have a heterogeneous mix of vessels) experience greater deviations in fuel consumption from the benchmark expected fuel consumption based on the assumption that the route is served by the same type of vessel. For the reader's convenience, we also report the summary of other parameters (ε, β_k, $\kappa_i jt$) in Table 5 and Figure 6 required to evaluate the effects of IMO2023, which we do in the next Section.

Table 5: Model Parameters

	(1:OLS)	(2:IV)
ε	-7.298^{***}	-10.299^{***}
	(0.561)	(2.181)
β_k	-0.041^{***}	-0.030^{***}
	(0.011)	(0.009)
ϕ^* with $\frac{\partial \kappa}{\partial s_{ij}} \neq 0$	1.176^{***}	1.118^{***}
	(0.038)	(0.042)
ϕ^* with $\frac{\partial \kappa}{\partial s_{ij}} = 0$	1.130^{***}	1.165^{***}
	(0.021)	(0.060)

Note: Standard errors are in parentheses; ϕ^* standard errors come from the Fisher Information Score.
$^{***}p < 0.01$; $^{**}p < 0.05$; $^{*}p < 0.1$

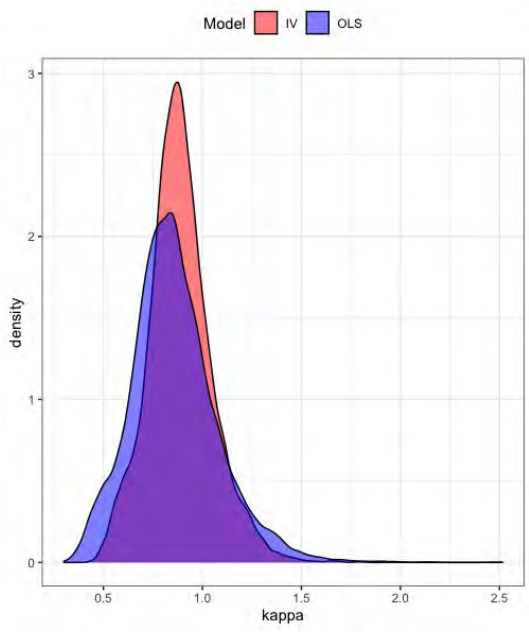

Figure 6: $\kappa(s)$ Distributions

5 The Effect of IMO2023 on Liner and Air Transportation

As discussed in Section 2, IMO2023 will force containerized fleet to slow down. The slowdown will effectively decrease its capacity: In Section 2.2, we calculated it as a proportional decrease from each country j to the U.S., $\underline{\omega}_j$.[38] Our model predicts that, in response to this capacity decrease, the air transportation to the U.S. will increase: We label the proportional change in air transportation as $\overline{\omega}_{ij}$. Furthermore, slower delivery of non-perishables will also decrease their utility to consumers: We denote this decrease with v ($1 \geq v \geq 0$). With this notation, the utility function of the first post-post year T (i.e., $T = 2023$) can then be written in terms of the pre-reform year $t = 2019$ keeping the consumption of the numeraire good constant:

$$U_{iT} = q_{0,it}^{1-\mu} \left[\sum_j \left(v_j \kappa_{it} \kappa_j (\underline{\omega}_j \underline{q}^*_{ijt})^{\frac{\varepsilon-1}{\varepsilon}} + \overline{\omega}_{ij} \overline{q}_{ijt}^{\frac{\varepsilon-1}{\varepsilon}} \right) \right]^{\mu \frac{\varepsilon}{\varepsilon-1}},$$

We use the color blue for the post-reform multipliers, which we already know, and the color red for those that we still need to identify. Using our estimates of β_k and our calculated slowdown values $\underline{\rho}_j$ from equation (8), we calculate the value of v_j as:

$$v_j \equiv= \left(\frac{TIME_{ijT}}{TIME_{ijt}} \right)^{\beta_k} = \left(\frac{\frac{1}{\underline{\rho}_j} TIME_{ijt}}{TIME_{ijt}} \right)^{\beta_k} = \underline{\rho}_j^{-\beta_k}.$$

Changes in the shipping capacity and preferences for non-perishables will likely affect the equilibrium ocean freight rate. We define the proportional change as: $\underline{\alpha}_{ij} = \underline{f}_{ijT} / \underline{f}_{ijt}$. Depending on the air transportation supply function, the air freight rate may also be affected. To accommodate for such a possibility, we model an increase in air transportation as a function of the increase in the liner freight rate as follows:

$$\overline{\alpha}_{ij} \equiv \overline{f}_{ijT} / \overline{f}_{ijt} = (1 + \zeta(\underline{\alpha}_j - 1)) \qquad \zeta \geq 0.$$

[38] By construction, $1 \geq \underline{\omega}_j \geq 0$. Due to data limitation, we aggregate it to the country-exporter j, thus assuming that the quantity restriction will be the same across all importing regions i in the U.S. for all exports from j.

In our quantitative assessment, we will consider two scenarios: (i) flat air transportation supply curve ($\zeta = 0$); and (ii) $\zeta = \frac{1}{6}$.[39] In what follows, we use the previously identified structural parameters of the model to solve for $\underline{\alpha}_{ij}$, $\overline{\alpha}_{ij}$, and $\overline{\omega}_{ij}$. Our Identification Algorithm I relies on the fixed point argument and proceeds in the following steps. $\underline{\alpha}_{ij}$, $\overline{\alpha}_{ij}$, and $\overline{\omega}_{ij}$.

Identification Algorithm I:

(Step 1) Compute an updated $K_i^0(\underline{\omega}_j, v_{ij})$: $K_i^0(\underline{\omega}_j, v_{ij}) = \frac{1-\mu}{\mu}\left[\sum_{j=1}^N v_{ij}\kappa_j\kappa_{it}(\underline{\omega}_j\underline{q}_{ijt})^{\frac{\varepsilon-1}{\varepsilon}} + \overline{q}_{ijt}^{\frac{\varepsilon-1}{\varepsilon}}\right]$.

(Step 2) Compute $\underline{\alpha}_{ij}$ as: $\underline{\alpha}_{ij} = \frac{\Gamma(\underline{\omega}_j, v_{ij}, \underline{\alpha}_{ij})(\underline{\tau}_{ijt} + \underline{f}_{ijt}/\underline{p}_{jt}) - \underline{\tau}_{ijt}}{\underline{f}_{ijt}/\underline{p}_{jt}}$, where $\Gamma(\underline{\omega}_j, v_{ij}, \underline{\alpha}_{ij})$ is the proportional change in the ad-valorem trade costs of non-perishables, which, using equation (11), is computed as follows: $\Gamma(\underline{\omega}_j, v_{ij}, \underline{\alpha}_{ij}) = \frac{\underline{\tau}_{ijt} + \underline{\alpha}_{ij}\underline{f}_{ijt}/\underline{p}_{jt}}{\underline{\tau}_{ijt} + \underline{f}_{ijt}/\underline{p}_{jt}} = \underline{\omega}_j^{-\frac{1}{\varepsilon}}\frac{v_{ij}K_{it}}{K_i^0(\underline{\omega}_j, v_{ij})}$.

(Step 3) Calculate $\overline{\alpha}_{ij}$ as $\overline{\alpha}_{ij} = (1 + \zeta(\underline{\alpha}_{ij} - 1))$.

(Step 4) Using eq. (11), compute the proportional change in the demand for air transportation as:

$$\overline{\omega}_{ij} = \left(\frac{K_i^0(\underline{\omega}_j, v_{ij})}{K_{it}} \times \frac{\overline{\tau}_{ijt} + \overline{\alpha}_{ij}\overline{f}_{ijt}/\overline{p}_{ijt}}{\overline{\tau}_{ijt} + \overline{f}_{ijt}/\overline{p}_{ijt}}\right)^{-\varepsilon}.$$

(Step 5) Update K_i^0 to K_i^{0+1} using new air quantity: $K_i^{0+1} = \frac{1-\mu}{\mu}\left[\sum_j v_{ij}\kappa_j\kappa_{it}(\underline{\omega}_j\underline{q}_{ijt})^{\frac{\varepsilon-1}{\varepsilon}} + (\overline{\omega}_{ij}\overline{q}_{ijt})^{\frac{\varepsilon-1}{\varepsilon}}\right]$.

(Step 6) Check if $\sum_i |K_i^{n+1} - K_i^n| / \sum_i K_i^n < \delta^{\text{stop}}$ If yes, it means we found a sufficiently close approximation of $\overline{\omega}_{ij}$. If not, repeat steps 1-6 until convergence.

Calculating Carbon Emissions. We assume that each air route emits 1439.49 g CO_2 per ton-mile as per Shapiro (2016).[40] We calculate air distance as the great circle distance between custom district i and country j.[41] As for containers, we use an average observed g CO_2 per ton mile rating per route based on our shipping data. We use mileage estimates derived from BlueWater's rotation schedule. The average across routes is 10 g CO_2 per ton mile.

[39] $\zeta = \frac{1}{6}$ is consistent with the 2021 dynamics of freight rates (www.aircargonews.net).

[40] Shapiro uses the International Air Transport Association (IATA)'s 2009 fuel economy of air freight transport of 985.97 g CO_2/ton-km; we convert this figure to ton-miles. See Shapiro's Online Appendix A.4 for further details.

[41] We use CEPII's country j coordinates.

Finally, for both modes, we combine the change in container capacity ($\underline{\omega}_j$) and the change in air capacity ($\overline{\omega}_j$) with 2019 trade volume in tonnes transported by respective mode. Combining mode carbon efficiency (g CO_2 per ton-mile) with mode mileage (miles) and mode volume (tons) allows us to calculate total emissions levels before and after IMO2023.

5.1 Results and Discussion

We calculate results for six scenarios: with and without adjustments in κ (time-sensitivity preferences for containerized imports) and with three types of adjustment of air transportation to IMO2023. The results are presented in Table 6.2. In all six scenarios, liner capacity decreases by 6.6%, liner emissions decrease by 13.2%, and liner freight rate increases (ranging between 10.2% and 11.8%). Moreover, each IMO2023 scenario has a materially adverse effect (between \$4.8 and \$8.8 bln) on U.S. consumer surplus, which dwarfs any welfare changes from net emissions.[42] For welfare calculations, we assume that the social marginal cost of CO_2 is 40 USD per tonne. If we assume a higher marginal cost—see EPA (2022) recommended 2020 base year figures that range from 120 to 340 USD per metric tonne as a function of higher to lower discount rates—only the *magnitude*, not the *direction* of, the welfare estimate changes. Since net emissions increase for all scenarios that account for inter-modal substitution, higher CO_2 marginal cost estimates will *exacerbate* welfare losses that come from increased net emissions. Specifically, from Table 6.2's scenarios (1) and (4), the welfare-neutral value of CO_2 abatement (i.e., the marginal social cost of carbon that exactly offsets consumer welfare loss from less trade) would range between $\frac{\text{7,656 mil USD}}{\text{1.9 mil tonne of CO}_2} = 4530$ USD/tonne and $\frac{\text{8,884 mil USD}}{\text{1.69 mil tonne of CO}_2} = 5257$ USD/tonne. These welfare-neutral values are at least one order of magnitude larger than even the highest estimates of carbon's social cost.

Scenarios (1) and (4) are the most restrictive scenarios we consider as we artificially shut down possible substitution into air shipping. Therefore, by construction, there is zero effect of IMO2023 on net emissions by air transportation. These are the *only* scenarios in which IMO2023 successfully leads

[42] Please see Online Appendix A.3 for the derivations of consumer surplus and welfare changes.

Table 6: IMO2023 U.S. Imports Predicted Results (OLS $\varepsilon = 7.3$)

Scenario	(1)	(2)	(3)	(4)	(5)	(6)
Adjust κ?		No			Yes	
Air Pass Through (ζ)	0	1/6	0	0	1/6	0
%Δ Container Capacity	-6.57	-6.57	-6.57	-6.57	-6.57	-6.57
%Δ Air Capacity	0.00	32.99	33.84	0.00	40.99	42.67
%Δ Container Freight Rates	11.82	10.47	10.47	11.77	10.21	10.23
%Δ Air Freight Rates	0.00	1.52	0.00	0.00	1.49	0.00
%Δ Container Emissions	-13.21	-13.21	-13.21	-13.21	-13.21	-13.21
%Δ Air Emissions	0.00	33.30	34.03	0.00	41.33	42.71
Net %Δ Emissions	-3.48	21.05	21.58	-3.48	26.95	27.97
Net Δ Emissions (mil tonne)	-1.69	10.24	10.49	-1.69	13.11	13.60
CO_2 Welfare (mil USD)	68	-409	-420	68	-524	-544
Δ Consumer Surplus (mil USD)	-7656	-4830	-4762	-8884	-5279	-5144
Net Δ Welfare (mil USD)	-7588	-5239	-5182	-8816	-5803	-5688

to combined air and liner emissions reduction (-3.5%). In all remaining scenarios where substitution is allowed, net combined emissions increase!

As discussed before, emissions increase for two reasons. First, limiting liner capacity naturally increases liner freight rates and, by extension, the relative liner-to-air freight rate. As a result, the relative and the absolute quantity of air-shipped goods increases. And since air shipping is two orders of magnitude more carbon-intensive than liner shipping, small changes in modal choice can quickly lead to a net emission increase. If we focus our attention only on the “freight rate" channel, combined net emissions increase by 21 to 22%, as reported by columns (2) and (3). Second, slower delivery of imported goods by liner shipping decreases consumer utility from these goods, thus increasing air-shipped imports even more. With this effect, columns (5) and (6) show that combined net emissions increase by 27 to 28%!

Our results raise the following question: Why would the IMO propose a reform that could increase combined liner and air carbon emissions and decrease consumer surplus? The answer to this question consists of at least two parts. First, the IMO is tasked with a narrow goal of reducing ocean-transportation emissions only, and IMO2023 does precisely that: in all six scenarios above,

liner emissions do decrease. Second, given that the IMO consists of the representatives of carriers, shipbuilders, and shipping-related bankers, IMO2023 satisfies other agency-specific goals, such as (i) increasing short-run profits of carriers and (ii) increasing the demand for new vessels in the medium and long run.

Indeed, as indicated in our all-inclusive scenarios by columns (5) and (6), carriers' revenue will immediately increase by 3.7%. Corresponding profits will increase by at least as much since, amid increasing revenue, the carrier's cost will decrease due to (i) lower transportation volumes and (ii) lower marginal cost of transportation at a lower speed. The shipbuilding sector can expect more orders to restore the shipping capacity, and bankers will face a greater demand for shipbuilding financing. To summarize, in addition to decreasing ocean-only carbon emissions, IMO2023 will also benefit the industry by engineering profit opportunities for all participants.

A broader conclusion from IMO2023 is that specialized agencies are likely to focus only on agency-specific goals when in charge of regulatory activities.[43] Reorganizing the U.N. or coordinating policies across U.N. agencies is no simple task. However, the U.N. can task specialized agencies with broader goals, which is likely to achieve better policy-consistent outcomes. We explore this scenario in the next Section.

6 An Alternative Policy Instrument: Fuel Taxes and Subsidies

In this Section, we evaluate an alternative policy of regulating air and liner transportation emissions by means of taxes or subsidies imposed only on liner transportation. We focus on this particular type of policy for three reasons. First, as we mentioned above, reorganizing U.N. or coordinating its policies across units might be prohibitively difficult. Therefore, we consider a policy that the IMO could plausibly and unilaterally oversee. Second, we explore taxes/subsidies rather than quantitative restrictions because these are widely used policy tools applied to environmental regulation in many contexts. Furthermore, one of the largest liner carriers, Maersk, voiced its discontent with

[43] Within the U.N., there are different entities considering environmental policies for liner shipping, air travel, production, etc.

IMO2023 and proposed an alternative in the form of a carbon tax of 150 dollars per tonne of CO_2 (Wittels, 2021), so this is also a policy considered by market participants. Finally, tax instruments will facilitate an apples-to-apples comparison with IMO2023 which regulated only ocean shipping.

Motivated by these considerations, we utilize our framework and data to evaluate the efficiency of imposing carbon taxes and subsidies on maritime shipping. Carbon taxes effectively act as fuel taxes: for a given carbon tax expressed in dollars per tonne of emitted CO_2, we use the carbon content of a fuel product to convert the carbon tax into a fuel tax. From the carrier's perspective, a fuel tax increases the marginal costs of transportation. In the model with the endogenous speed choice in Section 3.2, a higher marginal cost will (i) induce a slowdown by the carrier compared to the original equilibrium, thus decreasing the utility from the ocean-transported imports and (ii) will increase the final price of ocean-transported imports. Both channels will have a negative effect on the quantity of ocean-transported imports and cause more substitution towards air-transported imports. By contrast, subsidizing fuel will cause the opposite effects. Maritime fuel subsidies can be thought of as vessel-based "carbon" subsidies: we interchange our use of language between fuel and carbon subsidies. We proceed with quantifying tax instruments impacts using our model with endogenous speed by liner carriers (Section 3.2). We organize this section by describing how we solve our model with a carbon tax, followed by results and discussion.

6.1 Simulating fuel taxes and subsidies

In this section, we simulate the short-run, partial equilibrium impact of bunker costs on carbon emissions for liner carriers. We apply the following formula to calculate the change in bunker cost from $b_0 = 432.30$ USD/tonne[44] to b_1 as a result of tax $\underline{\tau}_c$ expressed in USD per tonne of carbon:

$$b_1 = b_0 + \underline{\tau}_c \underline{\theta}_k,$$

[44] $b_0 = 432.30$ USD/tonne is the 2019 simple average of American bunker fuel rates based Clarksons's 2019 data.

where $\underline{\theta}_k$ is carbon content of bunker fuel.[45]

Our solution approach is conceptually similar to our previous **Identification Algorithm I** but with one key difference: liner carriers choose route speed in response to exogenous shocks such as fuel taxes or subsidies. The essential modification to **Identification Algorithm I** is to introduce an outer loop where liner carriers observe the current guess of K_{it} and choose their speed accordingly.

Identification Algorithm II:

(Step 0) Collect the pre-reform optimal speed $s_{ij}^* = \zeta_{ij}^* s_{ij}^{\mathrm{D}}$ calculated in Section 4.3's Calibration Step I. Use s_{ij}^* to compute the number of round trips for route ij, $n_{ij}(s_{ij}^*)$, based on equation (5). Next, compute $b_1(\underline{\tau}_c)$ for a given $\underline{\tau}_c$; and start iteration counter N. Initialize a guess on $K_{it}^N(\underline{\tau}_c)$ by setting $K_{it}^0(\underline{\tau}_c) = K_{it}(\underline{\tau}_c = 0)$.

(Step 1) Compute each route's new optimal route speed by finding the speed that maximizes route profits taking $K_{it}^N(\underline{\tau}_c)$ into account, namely: $s_{ij}^N \equiv s_{ij}(K_{it}^N(\underline{\tau}_c)) \in \arg\max \pi(K_{it}^N(\underline{\tau}_c))$ using equation (17) as a guide. Once again, compute the number of round trips as a function of speed, $n_{ij}^N(s_{ij}^N)$, using equation (5). Define container capacity change as the ratio of new round trips $n_{ij}^N(s_{ij}^N)$ to the pre-reform round trip count $n_{ij}(s_{ij}^*)$: $\underline{\omega}_{ij}^N = n_{ij}^N(s_{ij}^N)/n_{ij}(s_{ij}^*)$.

(Step 2) Use $\underline{\omega}_{ij}^N$ and run the **Identification Algorithm I** in Section 5 until convergence. After this inner loop converges, use $\underline{\omega}_{ij}^N$ and newly obtained $\overline{\omega}_{ij}^N$ to compute $\widehat{K_{it}^N}(\underline{\omega}_{ij}^N, \overline{\omega}_{ij}^N; \underline{\tau}_c)$.

(Step 3) Check if $\sum_i |\widehat{K_{it}^N}(\underline{\omega}_{ij}^N, \overline{\omega}_{ij}^N; \underline{\tau}_c) - K_{it}^N(\underline{\tau}_c)| / \sum_i K_{it}^N(\underline{\tau}_c) < \delta^{\text{stop}}$. If yes, this means that we have a sufficiently close approximation of $\boldsymbol{\omega} = (\underline{\omega}_{ij}, \overline{\omega}_{ij})$. If no, then iterate N forward, recompute speed and the corresponding capacity reduction via $\underline{\omega}_{ij}^{N+1} = n_{ij}^{N+1}\left(s_{ij}\left(\widehat{K_{it}^N}(\underline{\omega}_{ij}^N, \overline{\omega}_{ij}^N; \underline{\tau}_c)\right)\right)/n_{ij}(s_{ij}^*)$. Repeat steps 1-3 until convergence.

[45] We use $\underline{\theta}_k = 3.14$ grams of CO_2 per grams of fuel. We arrive at this number by taking a simple average of annual CO_2 emissions relative to annual fuel consumption over all containerships in our THETIS sample.

6.2 Results

Using Algorithm II and focusing on U.S. imports, we can predict the effect of the carbon tax imposed on liner transportation ($\underline{\tau}_c$) on the *joint* air and liner transportation emissions. We apply Algorithm II to each in the following range:

$$\underline{\tau}_c \in [-100, -99, -98, ..., -1, 0, 1, ..., 98, 99, 100],$$

where positive values of $\underline{\tau}_c$ denote carbon taxes and negative ones denote subsidies.

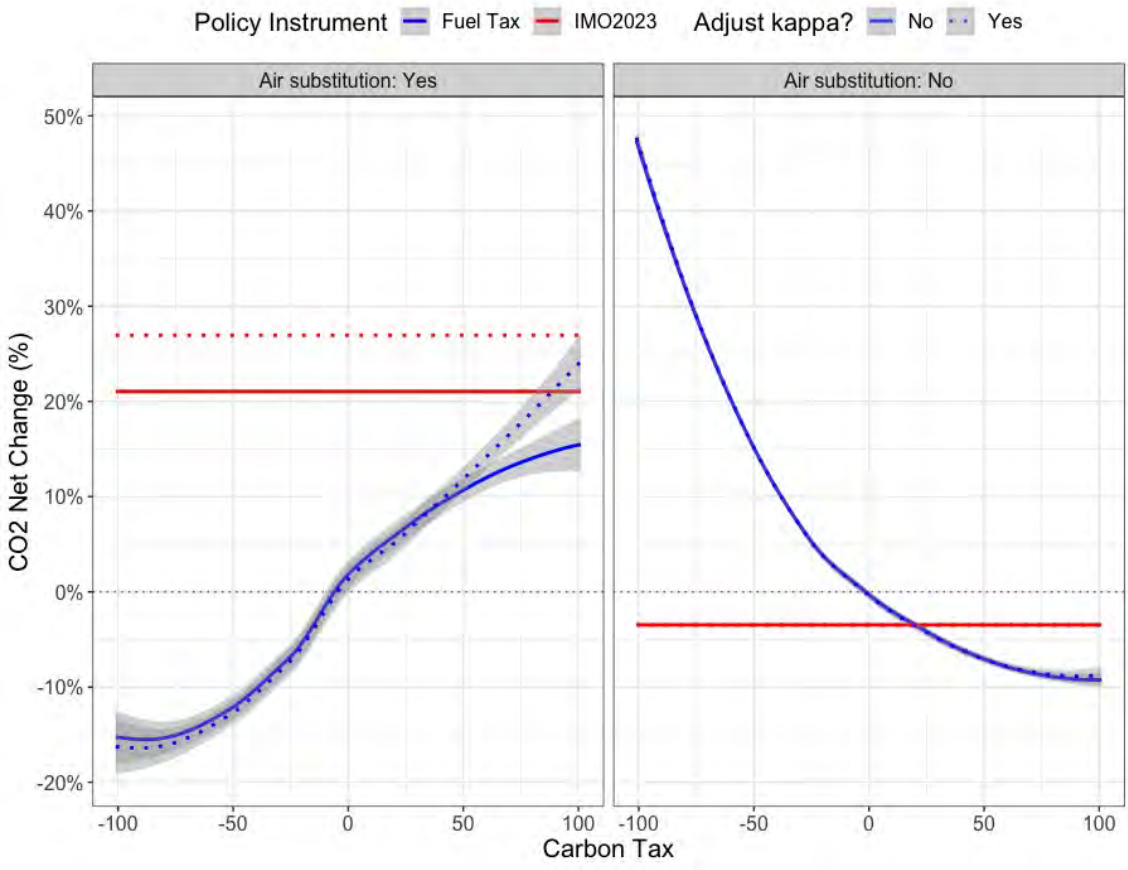

Figure 7: Carbon tax vs IMO2023 comparison (OLS $\varepsilon = 7.3$)

Our results are presented in Figure 7. The left panel presents results with liner-to-air substitutability. It shows that all "carbon subsidies" to liner shipping decrease joint net emissions, whereas carbon taxes have the opposite effect. These seemingly counter-intuitive results emanate from the

liner-to-air substitutability: subsidizing liner shipping decreases air shipping, which is much more carbon-intensive than liner shipping.[46] Instead, if we artificially eliminate intermodal substitution, as we do in the right panel of Figure 7, we get the exact opposite results: subsidizing (taxing) liner shipping to move faster (slower) without any change from air freight leads an increase (decrease) in joint emissions.

To explain the intuition of this result, we use a subsidy of $\underline{\tau}_c = -\$40$ as an example. Specifically, we calculate how this subsidy will affect various aspects of liner and air shipping as well as consumer surplus, very much akin to our analysis of IMO2023. These results are presented in Table 7. As in IMO2023 Table , columns (1) and (4) present scenarios results where there is no substitution between air and liner transportation, while all other columns allow for such substitution. In all scenarios, subsidizing liner fuel will: (i) spur liner carriers to speed up, thus increasing their effective capacity (while keeping the number of vessels fixed); (ii) decrease liner freight rate; and (iii) increase emissions from liner transportation. In scenarios (1) and (4), joint (air and liner) net emissions will also increase since, by construction, they are only affected by liner emissions.

[46] In Figure 7, we also show the effects of IMO2023 on joint emissions. Specifically, they are denoted by the red horizontal lines. Note that, with substitutability, taxing liner carbon emissions, while counterproductive, is less harmful than IMO2023.

Table 7: Fuel subsidy of \$40 per tonne of CO_2 imposed on containerized imports (OLS $\varepsilon = 7.3$)

Scenario	(1)	(2)	(3)	(4)	(5)	(6)
Adjust κ?		No			Yes	
Air Pass Through (ζ)	0	1/6	0	0	1/6	0
%Δ Container Capacity	9.62	10.18	10.18	9.77	10.36	10.36
%Δ Air Capacity	0.00	-33.63	-33.67	0.00	-34.59	-34.63
%Δ Container Freight Rates	-9.92	-11.11	-11.12	-9.86	-11.06	-11.05
%Δ Air Freight Rates	0.00	-0.23	0.00	0.00	-0.23	0.00
%Δ Container Emissions	35.18	37.49	37.49	35.44	37.86	37.87
%Δ Air Emissions	0.00	-34.11	-34.14	0.00	-34.99	-35.03
Net %Δ Emissions	9.27	-15.24	-15.26	9.34	-15.79	-15.82
Net Δ Emissions (mil tonne)	4.51	-7.41	-7.42	4.54	-7.68	-7.69
CO_2 Welfare (mil USD)	-180	296	297	-182	307	308
Δ Consumer Surplus (mil USD)	567	421	421	580	435	435
Net Δ Welfare (mil USD)	387	717	718	399	742	742

However, when liner-to-air substitutability is allowed, faster and cheaper liner shipping will decrease the quantity of air-transported imports. Since air transportation is much more carbon intensive than liner transportation, this decrease will be sufficient to counteract increased liner emissions: in the end, net joint emissions are negative! Finally, since there is an increase in the total volume of trade delivered with lower freight rates, the net welfare effect for the US will also be positive in all scenarios.

To conclude, taxing/subsidizing carbon emissions in our context is a more efficient tool than quantitative restrictions proposed by IMO2023, even if, as in the case of IMO2023, these tools are applied only to liner shipping. Specifically, subsidizing carbon emissions in liner shipping allows to decrease joint net emissions through the reverse leakage from air to liner shipping. Therefore, if tasked with a broader goal, IMO alone can decrease joint net emissions by regulating liner shipping only.

7 Conclusion

In this paper, we show that the mechanism proposed by IMO2023 will lead to unintended consequences: carbon leakage into air transportation. This leakage will cause the joint emissions from air and liner transportation to increase. Thus, even though a narrow IMO goal—to decrease ocean transportation emissions—is achieved, the reform will be counterproductive if we consider a broader goal of reducing joint emissions from transportation. Instead, we show that a carbon subsidy to liner shipping would decrease joint emissions through the reverse leakage of emissions from air-to-liner shipping. Our analysis highlights the problem of assigning responsibility for different sectors to different government units, which may or may not interact with each other. Under these circumstances, one needs to task these agencies with broader goals.

References

Adina Ardelean and Volodymyr Lugovskyy. It Pays to Be Big: Price Discrimination in Maritime Shipping. Technical report, 2023.

Jose Asturias. Endogenous Transportation Costs. Mimeo, Georgetown University Qatar, 2019.

Randy Becker and Vernon Henderson. Effects of air quality regulations on polluting industries. *Journal of Political Economy*, 108(2):379–421, 2000. doi: 10.1086/262123. URL https://doi.org/10.1086/262123.

Marc F Bellemare, Takaaki Masaki, and Thomas B Pepinsky. Lagged explanatory variables and the estimation of causal effect. *The Journal of Politics*, 79(3):949–963, 2017.

Tibor Besedeš and Antu Panini Murshidb. Experimenting with ash: The trade-effects of airspace closures in the aftermath of eyjafjallajökull. *Mimeo*, 2022.

Timothy Besley, Thiemo Fetzer, and Hannes Mueller. The welfare cost of lawlessness: Evidence from somali piracy. *Journal of the European Economic Association*, 13(2):203–239, 2015.

Bruce A. Blonigen and Wesley W. Wilson. Port Efficiency and Trade Flows. *Review of International Economics*, 16(1):21–36, February 2008.

Lucy Budd and Stephen Ison. The role of dedicated freighter aircraft in the provision of global airfreight services. *Journal of Air Transport Management*, 61:34–40, 2017. ISSN 0969-6997. doi: https://doi.org/10.1016/j.jairtraman.2016.06.003. URL https://www.sciencedirect.com/science/article/pii/S0969699715301642. Special Issue on Air Cargo: A By-Product or Success Factor?

Brian R Copeland. Pollution content tariffs, environmental rent shifting, and the control of cross-border pollution. *Journal of International Economics*, 40(3):459–476, 1996. ISSN 0022-1996. doi: https://doi.org/10.

1016/0022-1996(95)01415-2. URL https://www.sciencedirect.com/science/article/pii/0022199695014152. Symposium on Growth and International Trade: Empirical Studies.

Brian R. Copeland, Joseph S. Shapiro, and M. Scott Taylor. Chapter 2 - globalization and the environmentwe thank our discussants, clare balboni and david hemous, and participants in a handbook conference for excellent comments, kenneth lai for excellent research assistance, and nsf ses-1850790. In Gita Gopinath, Elhanan Helpman, and Kenneth Rogoff, editors, *Handbook of International Economics: International Trade, Volume 5*, volume 5 of *Handbook of International Economics*, pages 61–146. Elsevier, 2022. doi: https://doi.org/10.1016/bs.hesint.2022.02.002. URL https://www.sciencedirect.com/science/article/pii/S1573440422000028.

James J Corbett, Haifeng Wang, and James J Winebrake. The effectiveness and costs of speed reductions on emissions from international shipping. *Transportation Research Part D: Transport and Environment*, 14(8):593–598, 2009.

Anca Cristea, David Hummels, Laura Puzzello, and Misak Avetisyan. Trade and the greenhouse gas emissions from international freight transport. *Journal of Environmental Economics and Management*, 65(1):153–173, 2013. doi: 10.1016/j.jeem.2012.06.00. URL https://ideas.repec.org/a/eee/jeeman/v65y2013i1p153-173.html.

Kevin Cullinane and Mahim Khanna. Economies of scale in large container ships. *Journal of transport economics and policy*, pages 185–207, 1999.

Joshua Elliott, Ian Foster, Samuel Kortum, Todd Munson, Fernando Pérez Cervantes, and David Weisbach. Trade and carbon taxes. *American Economic Review*, 100(2):465–69, May 2010. doi: 10.1257/aer.100.2.465. URL https://www.aeaweb.org/articles?id=10.1257/aer.100.2.465.

EPA. *Report on the Social Cost of Greenhouse Gases: Estimates Incorporating Recent Scientific Advances*. September 2022. URL https://subscriber.politicopro.com/eenews/f/eenews/?id=00000184-77c6-d07e-a5fd-f7df41f80000. This document is *Supplementary Material for the Regulatory Impact Analysis for the Supplemental Proposed Rulemaking, "Standards of Performance for New, Reconstructed, and Modified Sources and Emissions Guidelines for Existing Sources: Oil and Natural Gas Sector Climate Review."*.

Jasper Faber, Maarten 't Hoen, Marnix Koopman, Dagmar Nelissen, and Saliha Ahdour. Estimated Index Values of New Ships. Analysis of EIVs of Ships That Have Entered The Fleet Since 2009. CE Delft 15.7E50.14, 2015.

Farid Farrokhi and Ahmad Lashkaripour. Can Trade Policy Mitigate Climate Change? Mimeo, indiana university, September 2021.

Sharat Ganapati, Woan Foong Wong, and Oren Ziv. Entrepôt: Hubs, Scale, and Trade Costs. Technical report, University of Oregon, 2020.

Michael Greenstone. The impacts of environmental regulations on industrial activity: Evidence from the 1970 and 1977 clean air act amendments and the census of manufactures. *Journal of Political Economy*, 110(6):1175–1219, 2002. doi: 10.1086/342808. URL https://doi.org/10.1086/342808.

Howard K Gruenspecht. Differentiated regulation: The case of auto emissions standards. *American Economic Review*, 72(2):328–31, 1982. URL https://EconPapers.repec.org/RePEc:aea:aecrev:v:72:y:1982:i:2:p:328-31.

Antonio Guterres. UN Secretary-General: "Making Peace with Nature is the Defining Task of the 21st century", Dec 2020. URL https://tinyurl.com/a74bwarn.

Rema Hanna. Us environmental regulation and fdi: Evidence from a panel of us-based multinational firms. *American Economic Journal: Applied Economics*, 2(3):158–89, July 2010. doi: 10.1257/app.2.3.158. URL https://www.aeaweb.org/articles?id=10.1257/app.2.3.158.

Jamie Hansen-Lewis and Michelle M Marcus. Uncharted waters: Effects of maritime emission regulation. Technical report, National Bureau of Economic Research, 2022.

Hercules E Haralambides. Gigantism in container shipping, ports and global logistics: a time-lapse into the future, 2019.

James Harrigan. Airplanes and comparative advantage. *Journal of International Economics*, 82(2):181–194, November 2010.

Inga Heiland, Andreas Moxnes, Karen-Helene Ulltveit-Moe, and Yuan Zi. Trade From Space: Shipping Networks and The Global Implications of Local Shocks. Technical report, 2022.

David Hummels, Volodymyr Lugovskyy, and Alexandre Skiba. The trade reducing effects of market power in international shipping. *Journal of Development Economics*, 89(1):84–97, May 2009.

David L. Hummels and Georg Schaur. Hedging price volatility using fast transport. *Journal of International Economics*, 82(1):15–25, September 2010.

David L. Hummels and Georg Schaur. Time as a Trade Barrier. *American Economic Review*, 103(7):2935–59, December 2013.

David L. Hummels and Alexandre Skiba. Shipping the good apples out? an empirical confirmation of the alchian-allen conjecture. *Journal of Political Economy*, 112(6):1384–1402, 12 2004.

IMO. Imo progress on revised ghg strategy, mediterranean eca adopted. *IMO Press Release*, December 2022. URL https://www.imo.org/en/MediaCentre/PressBriefings/pages/MEPC-79.aspx.

Jota Ishikawa and Nori Tarui. Backfiring with backhaul problems. *Journal of International Economics*, 111(C): 81–98, 2018.

Mark R. Jacobsen and Arthur A. van Benthem. Vehicle scrappage and gasoline policy. *American Economic Review*, 105(3):1312–38, March 2015. doi: 10.1257/aer.20130935. URL https://www.aeaweb.org/articles?id=10.1257/aer.20130935.

Brian G. Kinyua. Shipping's decarbonization outlook for 2023. *Maritime Executive*, January 2023. URL https://maritime-executive.com/editorials/shipping-s-decarbonization-outlook-for-2023.

Samuel Kortum and David A. Weisbach. Optimal Unilateral Carbon Policy. Technical report, 2021.

Paul R. Krugman. Scale economies, product differentiation, and the pattern of trade. *American Economic Review*, 70(5):950–59, December 1980.

Ahmad Lashkaripour and Volodymyr Lugovskyy. Profits, scale economies, and the gains from trade and industrial policy. *CAEPR Working Paper 2017-004*, 2022.

James R. Markusen. International externalities and optimal tax structures. *Journal of International Economics*, 5 (1):15–29, 1975. ISSN 0022-1996. doi: https://doi.org/10.1016/0022-1996(75)90025-2. URL https://www.sciencedirect.com/science/article/pii/0022199675900252.

Marc J. Melitz. The impact of trade on intra-industry reallocations and aggregate industry productivity. *Econometrica*, 71(6):1695–1725, November 2003.

Gabriela Mundaca, Jon Strand, and Ian R. Young. Carbon pricing of international transport fuels: Impacts on carbon emissions and trade activity. *Journal of Environmental Economics and Management*, 110:102517, 2021. ISSN 0095-0696. doi: https://doi.org/10.1016/j.jeem.2021.102517. URL https://www.sciencedirect.com/science/article/pii/S009506962100084X.

William Nordhaus. Climate clubs: Overcoming free-riding in international climate policy. *American Economic Review*, 105(4):1339–70, April 2015. doi: 10.1257/aer.15000001. URL https://www.aeaweb.org/articles?id=10.1257/aer.15000001.

Ian Parry, Mr Dirk Heine, Kelley Kizzier, and Tristan Smith. *Carbon taxation for international maritime fuels: Assessing the options*. International Monetary Fund, 2018.

Arthur Pigou. *The Economics of Welfare*. Macmillan, London, 1920.

Joseph S Shapiro. Trade costs, co2, and the environment. *American Economic Journal: Economic Policy*, 8(4): 220–54, 2016.

Powell Slaughter. Next year's carbon emissions standards could further complicate ocean shipping, May 2022. URL https://www.furnituretoday.com/supply-chain/next-years-carbon-emissions-standards-could-further-complicate-ocean-shipping/.

Anson Soderbery. Estimating import supply and demand elasticities: Analysis and implications. *Journal of International Economics*, 96(1):1–17, 2015. ISSN 0022-1996. doi: https://doi.org/10.1016/j.jinteco.2015.01.003. URL https://www.sciencedirect.com/science/article/pii/S0022199615000045.

Mark Szakonyi. Slow steaming, congestion to blunt container capacity injections: Zim, Aug 2021. URL https://www.joc.com/maritime-news/container-lines/zim-integrated-shipping-services/slow-steaming-congestion-blunt-2023-container-capacity-injections-zim_20210818.html.

Shinsuke Tanaka, Kensuke Teshima, and Eric Verhoogen. North-south displacement effects of environmental regulation: The case of battery recycling. *American Economic Review: Insights*, 4(3):271–88, September 2022. doi: 10.1257/aeri.20210201. URL https://www.aeaweb.org/articles?id=10.1257/aeri.20210201.

Peter Tirschwell. Slow-steaming hardly an emissions silver bullet. *Journal of Commerce Online*, May 2019. URL https://www.joc.com/maritime-news/container-lines/slow-steaming-hardly-emissions-silver-bullet_20190501.html.

USCG. Office of commercial vessel compliance (cg-cvc): International convention for the prevention of pollution by ships - marpol 73/78, 2022. URL https://www.dco.uscg.mil/Our-Organization/Assistant-Commandant-for-Prevention-Policy-CG-5P/Inspections-Compliance-CG-5PC-/Commercial-Vessel-Compliance/Domestic-Compliance-Division/MARPOL/.

Hulda Winnes, Linda Styhre, and Erik Fridell. Reducing ghg emissions from ships in port areas. *Research in Transportation Business & Management*, 17:73–82, 2015.

Jack Wittels. Maersk Seeks $150-a-Ton Carbon Tax on Shipping Fuel. *Bloomberg.com*, June 2:53–82, 2021.

Woan Foong Wong. The Round Trip Effect: Endogenous Transport Costs and International Trade. Technical report, University of Oregon, 2020.

Tianle Yuan, Hua Song, Robert Wood, Chenxi Wang, Lazaros Oreopoulos, Steven E Platnick, Sophia von Hippel, Kerry Meyer, Siobhan Light, and Eric Wilcox. Global reduction in ship-tracks from sulfur regulations for shipping fuel. *Science advances*, 8(29):eabn7988, 2022.

A Online Appendix—Not for Publications

A.1 Detailed Data Description

Technical characteristics of each vessel (vessel size, engine type, eco-equipment, design fuel consumption, etc.), which will allow us to predict speed changes to meet the required IMO 2023 CII. These data come from the *World Fleet Register* (WFR), maintained by Clarksons PLC—the world's leading shipbroker—and include all major commercial vessels.

Actual (observed) fuel consumption, distance traveled, and carbon emissions provided by THETIS-MRV (alternatively THETIS), an online, port state control/inspection database maintained by the European Maritime Safety Agency (EMSA). It was launched in August 2017 in an effort to support new owner reporting requirements pursuant to Regulation (EU) 2015/757 on Monitoring, Reporting, and Verification of CO_2 from marine transport. Regulation 2015/757 requires the owners to report carbon emissions per transport work for all vessels that (i) are larger than 5,000 gross tonnage (GT); and (ii) make at least one call to an EU territory port subsequent to January 1st, 2018. THETIS-MRV makes provisions for third party monitoring and verification of a ship owner's reported carbon emissions. THETIS-MRV's data on owner-reported technical efficiency is publicly available, and features annual emissions reports from 2018-2020.

There are roughly 15,000 unique IMO number-vessels in the THETIS-MRV database across 2018-2020. Our preferred efficiency rating is the Energy Efficiency Design Index (EEDI), which measures grams of CO_2 generated per ton-nautical mile. THETIS also records vessel Estimated Index Values (EIV). EIV ratings, relative to EEDI ratings, are: (i) better thought of as vessel design efficiency metric versus as a fuel efficiency rating; (ii) less data-intensive to calculate due to making simplifying assumptions about vessel operation; and (iii) tend to slightly overestimate EEDI ratings (Faber et al., 2015).

Data on container carriers, their service rotations and capacities on all routes worldwide between 2012 and 2020, provided by BlueWater Reporting. These data will allow us to determine the capacity and speed of liner transportation on importing routes to the U.S.

Matching different datasets. We link each vessel found in the THETIS-MRV registry back to the Clarksons' World Fleet Registry through the vessel's unique IMO number. The Clarksons-THETIS merge of the global liner fleet results in a match of 39.7% by count and 54.1% by capacity. The match is less than 100% because under THETIS carbon emissions were measured only from the vessels entering European ports, while Clarksons contains information about the entire global fleet. For comparison, the corresponding numbers for the bulk fleet are 42.3% and 38.5%, respectively. BlueWater Reporting contains all containerized maritime routes, which allows us matching (using IMO number) each containership present in either Clarksons or THETIS with its route in a given month.

A.2 Route Construction and Carrier Count

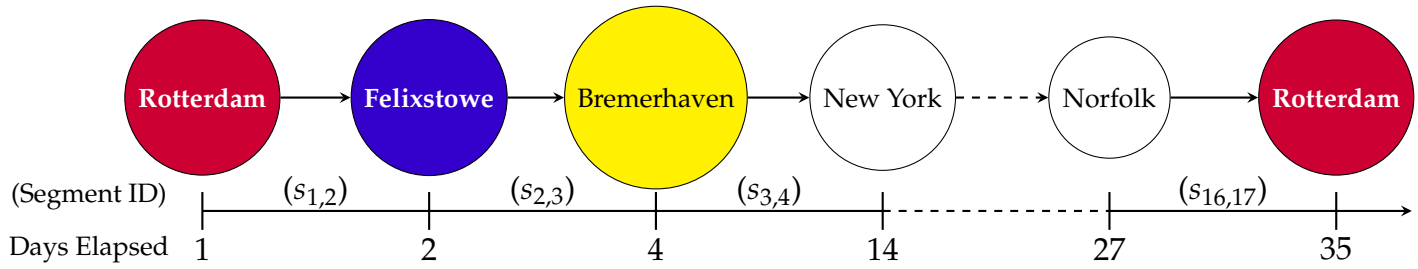

Figure A1: Container Rotation Example

Note: Port nodes are colored by country. Port to port pairs are identified by Segment ID $s_{i,j}$, where $i(j)$ indexes port stops (from stop i to stop j). Ports can be visited more than once whereas stop numbers are unique, e.g. Rotterdam is the 1st and 17th stop in the rotation. Finally, port stops between New York and Norfolk are excluded for illustrative simplicity. Carriers APL, CMA CGM, Hyundai, and Maersk Line service this rotation at various points throughout 2013.

A typical observation within BlueWater Reporting's historical rotation data lists the origin and destination port pair alongside the rotation that the pair belongs to. The rotation is a semi-colon separated string in the following form: "PortX 1 ; PortY 2" where a port name is followed by the number of days that have elapsed since the start of the rotation. In this way, a rotation can be thought of a sequence of port-to-port segments with a corresponding travel time given by the difference in the number of days elapsed. Additionally, each rotation lists the names of servicing carriers.

A BlueWater route is thus a sub-sequence of a larger rotation. The listed origin-destination pair, which serve as the endpoints of the route, *are not necessarily the endpoints* of a rotation. Moreover, BlueWater does not necessarily breakout all segments of a rotation. To put the problem in concrete terms, consider the example provided by Figure A1. BlueWater lists Rotterdam (origin port) to New York (destination port) as a route with the larger rotation. This rotation is serviced by four (4) carriers: APL, CMA CGM, Hyundai, and Maersk Line. Rotterdam (NL) to New York includes intermediate stops in Felixstowe (GB) and Bremerhaven (DE). Thus, there are at least four (4) carriers that serve New York from: the Netherlands; the United Kingdom; and Germany. However, BlueWater might *explicitly* report the four (4) carriers between the Netherlands and New York but not report the four (4) carriers between the United Kingdom and New York.

We clean our BlueWater rotation data to determine the number of carriers that service Country-US Custom District *routes* according to the following steps:

1. **Identify all unique ports across all rotations**. Port names are not necessarily unique. After cleaning, our sample includes 462 ports.

2. **Geo-code ports**. For each of the 462 ports, we determine the longitude/latitude coordinates.

3. **Map ports into countries and/or US Custom Districts**. Based on the port name and coordinates, we then map ports to countries. If the port is American, we further map the port into the relevant U.S. Custom district.

4. **Determine each rotation's total distance and time**. Since each rotation can be broken down into port-to-port pairs, we compute the sea distance traveled for each port pair.[47] Interestingly enough, at 3,769

[47] Besley et al. (2015) provides details about how to use GIS data and R to compute shortest paths over sea between port pairs.

unique pairs, the total number of unique port-to-port pairs is small relative to the theoretical maximum: $\frac{3{,}769}{462\times(461)/2} \approx 3.5\%$. Port pair travel time is based on the difference in total time elapsed. For example, Figure A1's segment $s_{3,4}$ implies a travel time of 10 days. Moreover, we calculate a sea distance of 4,230 miles (compared to the 4,000 mile estimate from SP PortWorld.

A.3 Additional Theoretical Derivations

A.3.1 Calculating changes in consumer surplus

IMO2023 is likely to impose economic cost on consumers. We will use the following procedure to evaluate the corresponding changes in consumer surplus. First, using demand functions (11), we will calculate pre-reform surplus on each route using the following formula:

$$CS_{it}^{pre} = \sum_j \int_0^{\underline{q}_{ijt}^{pre}} \left[\underline{\Lambda}_{ijt}\underline{q}_{ijt}^{-\frac{1}{\varepsilon}} - (\underline{p}_{ijt}^{pre}\underline{\tau}_{ijt}^{pre} + \underline{f}_{ijt}^{pre})\right] d\underline{q}_{ijt} + \sum_j \int_0^{\overline{q}_{ijt}^{pre}} \left[\overline{\Lambda}_{ijt}\overline{q}_{ijt}^{-\frac{1}{\varepsilon}} - (\overline{p}_{ijt}^{pre}\overline{\tau}_{ijt}^{pre} + \overline{f}_{ijt}^{pre})\right] d\overline{q}_{ijt}$$

where $\underline{\Lambda}_{ijt} = \frac{\kappa_{it}\kappa_j q_{0,it}}{K_{it}}$ and $\overline{\Lambda}_{ijt} = \frac{q_{0,it}}{K_{it}}$. Denoting our vector of post-reform changes as $\boldsymbol{\Omega}$, we express the ratio of post to pre utilities for i as:

$$U_{i,t+1}^{post}(\boldsymbol{\Omega}) \Big/ U_{it}^{pre} = \left[\sum_j \left(\kappa(\boldsymbol{\Omega})[\underline{q}_{ijt}(\boldsymbol{\Omega})]^{\frac{\varepsilon-1}{\varepsilon}} + [\overline{q}_{ijt}(\boldsymbol{\Omega})]^{\frac{\varepsilon-1}{\varepsilon}}\right)\right]^{\frac{\mu\varepsilon}{\varepsilon-1}} \Big/ \left[\sum_j \left(\kappa \underline{q}_{ijt}^{\frac{\varepsilon-1}{\varepsilon}} + \overline{q}_{ijt}^{\frac{\varepsilon-1}{\varepsilon}}\right)\right]^{\frac{\mu\varepsilon}{\varepsilon-1}},$$

and calculate changes in consumer surplus post reform as: $\Delta CS = \sum_{it} CS_{it}^{pre}\left(\frac{U_{it}^{post}(\boldsymbol{\Omega})}{U_{it}^{pre}} - 1\right)$.

A.3.2 Other welfare calculations

Welfare changes in transportation related to changes CO_2 emissions are more straightforward to quantify. Change in CO_2 emissions comes from evaluating:

$$\Delta CO_2 = \sum_{ij} \underline{q}_{ij}\underline{d}_{ij}(\underline{\omega}_{ij} - 1)(\underline{\xi}_{ij}^{post} - \underline{\xi}_{ij}^{pre}) + \sum_{ij} \overline{q}_{ij}\overline{d}_{ij}(\overline{\omega}_{ij} - 1)\overline{\xi}_{ij}$$

where $\underline{\xi}_{ij}^{post}$ ($\underline{\xi}_{ij}^{pre}$) is the amount of carbon generated per tonne-mile after (pre) reform for conatinerships; likewise, $\overline{\xi}_{ij}$ is the amount of carbon generated per tonne-mile for airplanes. Changes in net welfare are then $\Delta CS - \Delta CO_2 \times$ social cost of carbon.

A.4 Data Analysis of Shipping Speed and Route Stability

A.4.1 Coastal shipping time

To put our project into short term data context, we look at rotation time trends for U.S. routes broken down into importing coasts. The upshot of the figure is that whereas *scheduled* delivery time does change over time, underlying speed changes are relatively modest (e.g. ± 2 knots per hour).

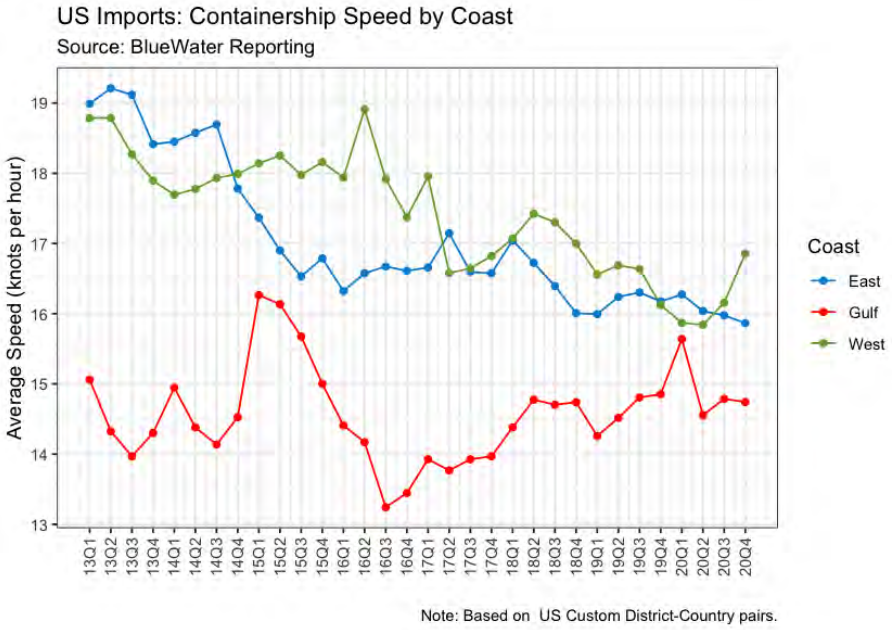

Figure A2: Shipping Speeds by Coast

Figure A2 depicts the average transit speed across country-custom district pairs per year. We segment custom districts into East, West, and Gulf Coast groupings. The East and West coast experienced a consistent decline in shipping speed. East Coast shipping speeds slowed by 31.3% on average [95% CI of -36.0% to -26.4%] and the West Coast experienced a similar decline of 25.8% [95% CI of -30.8% to -20.4%]. By contrast, Gulf Coast custom districts experienced more volatility in average shipping speed but no clear monotonic trend.

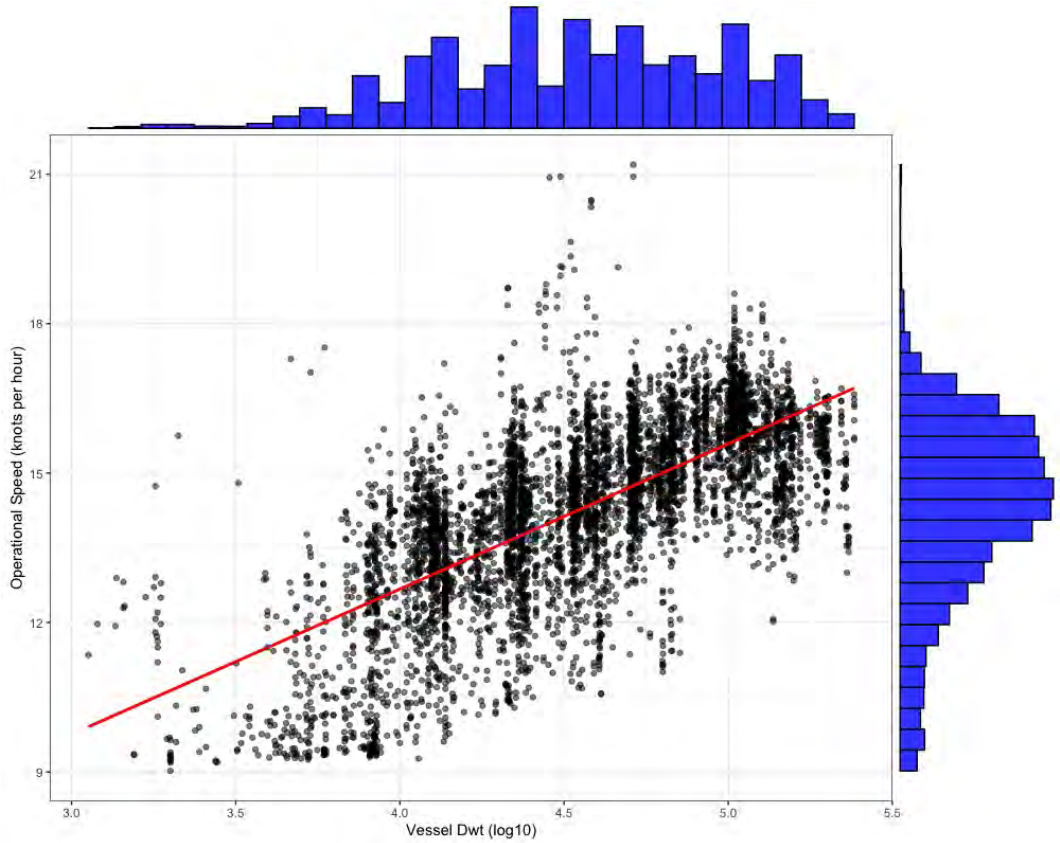

Figure A3: Average Vessel Size vs Speed
Source: Clarksons World Fleet Registry.

A.4.2 Route distance, time, and speed dispersion

At a conceptual level, fuel cost impacts will be affected by changes in route characteristics such as distance and or time. Carriers have multiple adjustment margins to choose from, ranging from different combination of ports to varying ship speeds. Whereas Figure A2 shows the average shipping time by *coast* over time, we now focus on *route* distance, time, and speed *dispersion*. For each year in our BlueWater 2013-2020 sample, we compute a route coefficient of variation:

$$CV_{ijt} = 100\% \times \frac{\sigma_{x_{ijt}}}{\mu_{x_{ijt}}}$$

where x is either route distance, transit time, and or speed. We next compute CV_{ijt}'s distribution and chart below:

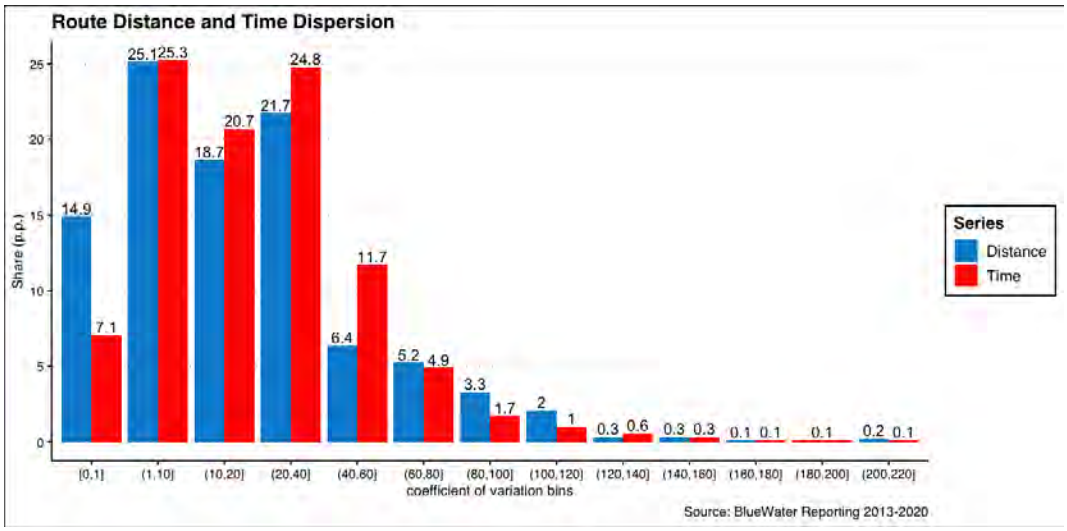

Figure A4: Distance and Time Dispersion Distribution

Since Figure A4 cannot speak directly to speed dispersion distribution, we construct an appropriate Figure A5 below:

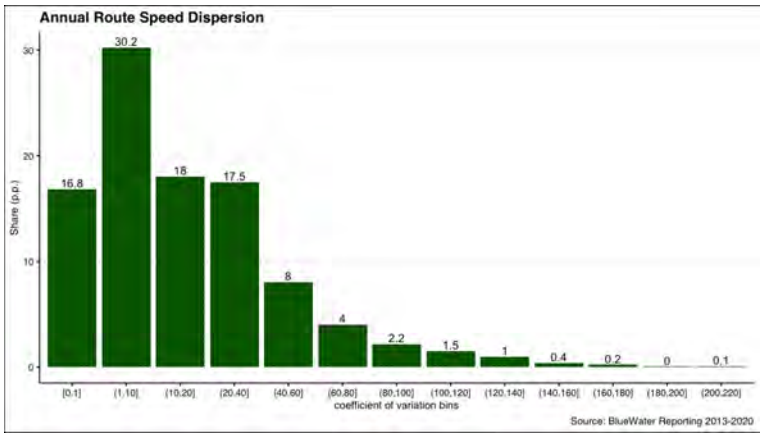

Figure A5: Speed Dispersion Distribution

Because we define a route as country-custom district pair, changes in route transit time might come from choosing different ports (e.g. different distance, possibly different time) or keeping the same ports but traveling at different speeds. We attempt to decompose and asses the importance of these two margins in the following way. The definition of velocity is $v = d/t$. Re-arranging yields $t = d/v$. Suppose that we have transit times for route ij, namely t_1 and t_0 such that $t_1 = t_0^{\alpha}$. In analogous fashion, we define new distance and velocity as $d_1 = d_0^{\beta}$ and $v_1 = v_0^{\theta}$. This leads arrangment allows us to write:

$$\frac{t_1}{t_0} = \frac{d_1/d_0}{v_1/v_0} \iff t_0^{\alpha-1} = d_0^{\beta-1} v_0^{-\theta+1}$$

Taking log of both sides yields:

$$(\alpha - 1)\log t_0 = (\beta - 1)\log(d_0) - (\theta - 1)\log(v_0) \tag{A19}$$

which provides us with estimating equation after we divide both sides by $(\alpha - 1)$.[48] Note that $|\beta - 1|$ and $|-(\theta - 1)|$ will give us some notion about the relative magnitudes of a distance effect compared to a speed effect on transit times.

We compute average route-carrier distance, transit time, and speed for two different time groupings: (i) monthly; and (ii) annually. Monthly data allows us to see which margins are more relevant for carriers in the short term whereas annual data gives us a better notion of long run adjustments. Our estimates of equation (A19) are provided by Table A1.

Results: Table A1 suggest that in the short run, carriers are more likely to change speed relative to distance, but this difference is statistically negligible. However, based on the annual estimates, it looks carriers' distance effect $(\beta - 1)$ (read: changing ports) tends to be modestly larger relative to the speed effect $(-\theta + 1)$ and this difference is statistically significant.

Table A1: Adjustment Margins models
Note: Dependent variable: $\log(t_1/t_0)$

	(1)	(2)	(3)	(4)	(5)	(6)
$(\beta - 1)$	1.029^{***}	1.029^{***}	1.029^{***}	0.958^{***}	0.958^{***}	0.955^{***}
	(0.014)	(0.014)	(0.009)	(0.017)	(0.017)	(0.013)
$(-\theta + 1)$	-1.039^{***}	-1.039^{***}	-1.038^{***}	-0.931^{***}	-0.930^{***}	-0.927^{***}
	(0.014)	(0.014)	(0.008)	(0.019)	(0.019)	(0.016)
$\left(\left\|\frac{(\beta-1)}{(-\theta+1)}\right\| - 1\right) \times 100\%$	-0.877	-0.879	-0.870	2.979^{**}	2.957^{**}	3.068^{***}
	(0.909)	(0.909)	(0.574)	(0.925)	(0.918)	(0.786)
R^2	0.818	0.818	0.820	0.794	0.796	0.833
nobs	315,931	315,931	315,931	25,269	25,269	25,269
Time Horizon	Month	Month	Month	Year	Year	Year
Fixed Effects	Route	Route + Carrier	Route × Carrier	Route	Route + Carrier	Route × Carrier

$^{***}p < 0.01$; $^{**}p < 0.05$; $^{*}p < 0.1$

A.4.3 Route Stability

We provide a distribution of two types of route stability measures. The first measure is route specific coefficient of variation of ports, or the ratio of the standard deviation of number of ports to the average number of ports: the higher the measure, the more (relatively) disperse the number of ports are on a given route. The second route stability measure is something we call "port share" and is defined as:

$$\frac{1}{|T_i||n_i|}\sum_{t_i \in T_i} n_i(t)$$

For each route i, T_i is the number of time periods that route i appears, n_i is the list of all ports ever used by route i, and $n_i(t)$ is the number of ports used by rotation i for month t. Using this measure, a score of zero (one) means no (perfect) port overlap for a given route.

Table A2 lists our stability results. On average, routes have close to a 20% coefficient of variation. Likewise, the average route uses roughly 60% of its ports in a given month. The average port share of roughly 60% suggests that at least on a short term basis, routes are fixed.

[48] We are ultimately interesting in testing the relative size of $|\beta - 1|$ vs $|-\theta + 1|$. For this reason, we are unbothered by the fact that are estimating $(\beta - 1)/(\alpha - 1)$ and $(-\theta + 1)/(\alpha - 1)$ rather than $(\beta - 1)$ and $(-\theta + 1)$.

Table A2: Route Stability Measures

Stat	Port Coefficient of Variation	Port Share
Min.	0.0%	15.4%
1st Qu.	6.9	43.5
Median	16.5	54.3
Mean	19.4	59.5
3rd Qu.	28.7	73.6
Max.	105.3	100.0